

# Comments from the reviewers:

## **Reviewer A:**

**”This article presents an assessment of passive microwave based soil moisture retrievals for irrigation detection. The manuscript is highly relevant and is written well.”**

### **Reply:**

We thank the reviewer for the general endorsement in publishing this manuscript and highly appreciate the detailed and constructive assessment.

---

**A.1. “Section 1.3: The obvious question here is why SMOS is not included in this list. After all, SMOS and SMAP use the L-band instrument, which is supposed to be more sensitive to soil moisture than C and X-band. I think it is essential that SMOS retrievals are included in this comparison for the sake of completeness. If SMOS does a poor job in detecting irrigation, that is also important to quantify and report.”**

### **Reply:**

We acknowledge that including soil moisture retrievals from SMOS would be a valuable addition to the manuscript. However, it is not absolutely integral to the completeness of this study. We think that this decision is supported by the following arguments:

- 1) Our efforts did not aim at conducting a comprehensive assessment of all current microwave soil moisture data sets with respect to irrigation quantification. Actually, our intention is to mainly discuss i) the difference between C-band and L-band, and ii) the difference between active and passive microwave remote sensing. For this reason, we included only three sensors, although with very different properties. For an intercomparison of the performance of various sensors with respect to soil moisture retrieval, we refer to existing literature (see point 2).
- 2) Soil moisture retrievals based on SMAP have repeatedly been shown to be more accurate than those based on SMOS [1,2].
- 3) The performance of SMOS soil moisture retrievals for irrigation quantification is thoroughly discussed in very recently published work [3]. In this paper, it was found that SMAP, ASCAT and AMSR-2 soil moisture outperform SMOS soil moisture with respect to rainfall estimation via SM2RAIN and that SMAP performs best overall. We argue that this is a viable indicator for the corresponding capabilities of the products in quantifying irrigation (since it can be simply added to precipitation), providing evidence that it is sufficient to solely include a single high quality L-band product.
- 4) Regarding the sensitivity of C- and L-band microwave observations to soil moisture, it has been shown that under certain conditions (e.g., dense vegetation cover), C-band soil moisture retrievals can be equally or even more accurate as L-band retrievals [4,5].

### **Changes in manuscript:**

We added the following sentence to anticipate the obvious question why SMOS is not included in the analysis:

Section 1.3, Page 8, Line 13:

“By using passive L-band and both active and passive C-band soil moisture data, we aim to assess the impact of the microwave observation frequency and the sensing technique with respect to irrigation quantification. For this reason we only used one dataset per category.”

**References:**

- [1] Colliander, A., Jackson, T. J., Bindlish, R., Chan, S., Das, N., Kim, S. B., ... & Asanuma, J. (2017). Validation of SMAP surface soil moisture products with core validation sites. *Remote sensing of environment*, 191, 215-231.
- [2] Chan, S. K., Bindlish, R., O'Neill, P. E., Njoku, E., Jackson, T., Colliander, A., ... & Yueh, S. (2016). Assessment of the SMAP passive soil moisture product. *IEEE Transactions on Geoscience and Remote Sensing*, 54(8), 4994-5007.
- [3] Brocca, L., Tarpanelli, A., Filippucci, P., Dorigo, W., Zaussinger, F., Gruber, A., & Fernández-Prieto, D. (2018). How much water is used for irrigation? A new approach exploiting coarse resolution satellite soil moisture products. *International Journal of Applied Earth Observation and Geoinformation*, 73, 752-766.
- [4] Al-Yaari, A., Wigneron, J. P., Ducharne, A., Kerr, Y. H., Wagner, W., De Lannoy, G., ... & Mialon, A. (2014). Global-scale comparison of passive (SMOS) and active (ASCAT) satellite based microwave soil moisture retrievals with soil moisture simulations (MERRA-Land). *Remote Sensing of Environment*, 152, 614-626.
- [5] van der Schalie, R., de Jeu, R., Parinussa, R., Rodríguez-Fernández, N., Kerr, Y., Al-Yaari, A., ... & Drusch, M. (2018). The Effect of Three Different Data Fusion Approaches on the Quality of Soil Moisture Retrievals from Multiple Passive Microwave Sensors. *Remote Sensing*, 10(1), 107.

---

**A.2. “Section 3.4: I am concerned about the use of the normal deviate based rescaling. As shown in Kumar et al. 2015 (HESS), when rescaling is performed relative to the model, it can lead to loss of information. I understand the need to have the datasets in a same space, but that can be done by scaling them using their own mean/standard deviations (see the strategy in Kumar et al. 2015). Using the model’s standard deviation for scaling will have a significant impact on the anomalies of the rescaled time series. These analysis should be redone without rescaling to the model’s mean/stdev.”**

**Reply:**

This is a very valuable criticism. However, apart from having the data in the same space, we do need the rescaling to correct for differing representative layer depths and spatial resolutions between products. It is true that the rescaling does have a significant impact on the anomalies, but we purposefully want that impact. Without the rescaling to the models mean and standard deviation, we could not justify a direct comparison of the irrigation estimates based on the respective soil moisture products.

Specifically, by matching the temporal mean and standard deviation of the satellite data sets to the model data set we correct for both horizontal and vertical systematic representativeness errors. This technique has been employed by various studies, e.g., [1,2]. In addition, we hereby implicitly compensate for different units (i.e., volumetric soil moisture

and degrees of saturation), which also avoids explicit conversion using (often inaccurate) auxiliary data (e.g., soil porosity maps).

**Changes in manuscript:**

None

**References:**

- [1] Dorigo, W., Scipal, K., Parinussa, R. M., Liu, Y. Y., Wagner, W., De Jeu, R. A., & Naeimi, V. (2010). Error characterisation of global active and passive microwave soil moisture data sets.
- [2] Albergel, C., De Rosnay, P., Gruhier, C., Muñoz-Sabater, J., Hasenauer, S., Isaksen, L., ... & Wagner, W. (2012). Evaluation of remotely sensed and modelled soil moisture products using global ground-based in situ observations. *Remote Sensing of Environment*, 118, 215-226.
- 

**A.3. “The assumption of a reliable model background is very key to this analysis. Generally the NLDAS2 data products are considered to be the “gold standard” over the US where the models are forced with precipitation data informed by gauge+radar information. The choice of MERRA2 is sub-optimal in my opinion. Why not use NLDAS2 datasets that are freely available, instead of MERRA2 (which is also coarser in spatial resolution)?”**

**Reply:**

It is true that the quality of the model soil moisture estimates is integral to the proposed methodology. However, most products, including NLDAS2, integrate observations of surface temperature and surface humidity. As outlined in [1] and [2], these observations are indirectly impacted by irrigation practices and hence implicitly alter soil moisture simulations. Although NLDAS2 would be a very suitable model choice in terms of quality, integrity and spatio-temporal resolution, we cannot employ it because near-surface air temperature and specific humidity are included in the forcing data [3].

**Changes in manuscript:**

None

**References:**

- [1] Wei, J., Dirmeyer, P. A., Wisser, D., Bosilovich, M. G., and Mocko, D. M.: Where Does the Irrigation Water Go? An Estimate of the Contribution of Irrigation to Precipitation Using MERRA, *Journal of Hydrometeorology*, 14, 275–289, <https://doi.org/10.1175/jhm-d-12-079.1>, <http://dx.doi.org/10.1175/JHM-D-12-079.1>, 2013.
- [2] Tuinenburg, O. and Vries, J.: Irrigation Patterns Resemble ERA-Interim Reanalysis Soil Moisture Additions, *Geophysical Research Letters*, 44, 2017.
- [3] <https://ldas.gsfc.nasa.gov/nldas/NLDAS2forcing.php>
-

**A.4. “Section 3.1.1: Since the article was submitted, SMAP released a new version of the data (including L3) that is supposed to have different bias characteristics, in particular. Normally I wouldn’t advocate chasing after different versions, but in this case, it is important to use this new version. Since the SMAP data formats haven’t changed, I assume this is relatively an easy thing to do.”**

**Reply:**

We thank you very much for pointing out the new version release. We collectively agree with you that it is crucial to use the updated SMAP Passive L3 V5 product. We investigated the impact of switching to V5 and found that the newer version indeed addresses the dry bias observed in V4. Moreover, the ascending and descending observations are more homogenous amongst each other. In the end, we re-processed all results using the SMAP V5 soil moisture data set.

**Changes in manuscript:**

First, we changed part of the data section to describe the key characteristics of V5.

**Section 3.1.1, Page 11, Line 4**

We used the L3\_SM\_P V5 data product, which is sampled at 36 km resolution. In this product version, a water body correction and an improved soil temperature depth correction have been applied, which have respectively reduced anomalous soil moisture values near large water bodies and the dry bias with respect to the SMAP core validation sites (Jackson, 2018). [1]

Moreover, all results (i.e., tables and plots) and numbers in the text were updated accordingly.

**References:**

[1][https://nsidc.org/sites/nsidc.org/files/technical-references/L2SMPE\\_Asmt\\_Rpt\\_EOPM\\_v5c\\_Jun2018.pdf](https://nsidc.org/sites/nsidc.org/files/technical-references/L2SMPE_Asmt_Rpt_EOPM_v5c_Jun2018.pdf)

---

**A.5. “Page 2, line 5: Correct the quotations – physically “ideal” amount”**

**Reply:**

Thank you for pointing that out, we have corrected the position of the leading quotation mark.

**Changes in manuscript:**

Section 1, Page 3, Line 5: “...physically “ideal” amount.”

---

**A.6. “Page 5, line 16: It’ll be good to briefly mention why the global maps differ.”**

**Reply:**

We agree that a brief discussion of the reasons for the substantial systematic deviations between different global irrigated area products is worthwhile.



**Changes in manuscript:**

Section 1.2.1, Page 6, Line 16

“However, there are large discrepancies between the different global data sets mainly stemming from varying definitions of irrigated areas among the data sets (i.e. area equipped for irrigation, irrigated area and cropped area), differences in the quality and spatial resolution of the input data sets and differing reference years (i.e., the years 2000 and 2005) (Salmon et al., 2015, Meier et al., 2018).”

**References:** [1] Meier, J., Zabel, F., & Mauser, W. (2018). A global approach to estimate irrigated areas—a comparison between different data and statistics. *Hydrology and Earth System Sciences*, 22(2), 1119-1133.

---

**A.7. “Page 6: With regard to thermal remote sensing, it’ll be good to include the Hain et al. JHM 2015 reference (https://journals.ametsoc.org/doi/full/10.1175/JHM-D-14-0017.1)”**

**Reply:**

We were not aware of this interesting work and regard it as a valuable addition to the paragraph focusing on thermal remote sensing approaches.

**Changes in manuscript:**

Section 1.2.1, Page 7, Line 9

“In contrast, Hain et al. [1] developed a novel method for inferring regions where non-precipitation inputs (e.g., irrigation) significantly impact terrestrial latent heat flux (LE). They compared modelled bottom-up LE (i.e., without irrigation) and top-down LE drawn from observations of diurnal land surface temperature changes which are connected to changes in the land surface moisture status and therefore irrigation.”

**References:**

[1] Hain, C. R., Crow, W. T., Anderson, M. C., & Yilmaz, M. T. (2015). Diagnosing neglected soil moisture source–sink processes via a thermal infrared–based two-source energy balance model. *Journal of Hydrometeorology*, 16(3), 1070-1086.

---

**A.8. “Page 7, lines 26-27, fix the quotations.”**

**Reply:**

We were not completely sure what was meant by this comment. We interpreted it as referring to a wrong position of the quotation and corrected it correspondingly.

**Changes in manuscript:**

Section 2.1, Page 7, Line 26-28

“The 2013 Farm and Ranch Irrigation Survey (FRIS) of the National Agricultural Statistics Service (NASS) of the USDA provides selected irrigation data from surveys conducted at approximately 35000 farms using irrigation across the US (USDA, 2013).”

---

**A.9. “Figure 2 caption: Please change SJF to SJV, NP to NPS”**

**Reply:**

Thank you very much for highlighting these errors. The caption of figure 2 now correctly attributes the abbreviations introduced for the focus regions.

**Changes in manuscript:**

Page 31, Figure 2: "...the Sacramento Valley (SV) and San Joaquin Valley (SJV) in the California Central Valley (CCV); Snake River Plain (SRP); Nebraska Plains (NPS), and the Mississippi Flood Plain (MFP)."

---

**A.10. "Page 10, Line 30: MERRA2 used a surface soil moisture layer of 5cm and not 10cm."**

**Reply:**

You are perfectly right. Unfortunately, due to a misleading rounding error in the Panoply viewer we assumed a 0.1 m surface soil moisture layer depth. Per default the software only seems to display 1 digit float values, so 0.05m was rounded up to 0.1m [1,2]. We were not aware of this default setting. Apart from updating Page 10, Line 30, this also impacts all results concerning irrigation quantification. Specifically, in the current rescaling formulation, this will directly reduce all IWU estimates by half and will be addressed in the revised manuscript version.

**Changes in manuscript:**

We have corrected Page 12, Line 8 to the actual layer depth of 5 cm. In addition, all IWU estimates were thus reduced by half and were updated accordingly.

**References:**

- [1] MERRA-2: File Specification (<https://gmao.gsfc.nasa.gov/pubs/docs/Bosilovich785.pdf>)
  - [2] Reichle, R. H., Draper, C. S., Liu, Q., Giroto, M., Mahanama, S. P., Koster, R. D., & De Lannoy, G. J. (2017). Assessment of MERRA-2 land surface hydrology estimates. *Journal of Climate*, 30(8), 2937-2960. (<https://journals.ametsoc.org/doi/10.1175/JCLI-D-16-0720.1>)
- 

**A.11. "Page 10, Lines 31-32: This statement is not strictly true. GLDAS for example, does not assimilate any screen level data."**

**Reply:**

Based on your comment we investigated the GLDAS (Version 2) assimilation scheme. According to the official website [1], a suite of atmospheric data sets are used to force the model. In version 2, the main inputs include the Princeton University meteorological forcing dataset [2], various precipitation data sets based on satellite observations and a range of land surface data sets. Specifically in [2], a summary of all the forcings used to construct the long term data set is given in Table 1. It can be seen that two of the five datasets include observations which can be altered by irrigation. The NCEP–NCAR reanalysis includes surface air temperature (T) and specific humidity (q) observations whereas CRU TS2.0 only includes T (assimilated from station observations). Hence, based on the here presented information, we cannot use GLDAS (V2) as an unbiased reference for the purpose of

irrigation quantification. Needless to say, we are open for other independent references concerning the GLDAS assimilation scheme.

**Changes in manuscript:**

We deleted the Examples “ERA-Interim” and “GLDAS” from the brackets on page 12, line 10.

**References:**

[1] <https://ldas.gsfc.nasa.gov/gldas/GLDASforcing.php>

[2] Sheffield, J., Goteti, G., & Wood, E. F. (2006). Development of a 50-year high-resolution global dataset of meteorological forcings for land surface modeling. *Journal of Climate*, 19(13), 3088-3111.

---

**A.12. “Figure 3 is nice. Can you show a difference map so it is easy to see where there are significant differences between rdry and rwet? The caption says ‘correlations are computed over agricultural areas only’. In that case, why is the map filled everywhere over CONUS?”**

**Reply:**

We thank you for stating that figure 3 proves valuable to the manuscript. As requested, we have added a difference map to the Appendix. Regarding the caption, thank you for pointing that out! The caption correctly states that the correlations are only computed over agricultural areas, however, the masking was not performed. Therefore, all other land regions were masked accordingly.

**Changes in manuscript:**

Page 32, Figure 3: The figures were correctly masked for agricultural land cover. Difference maps were added to the Appendix section (Figure A2).

---

**A.13. “Page 14, line 27: Is it a known fact that rice vegetation causes specular reflection? Any reference to back up this statement?”**

**Reply:**

Here, we carefully need to differentiate between different phenological development phases of rice. Between the actual establishment of the flood irrigation (the fields are usually covered with 10-15 cm of water) and the time when the rice starts to break through the water surface, we assume that specular reflection can be an issue (given low water surface roughness, i.e., low surface wind speeds). In the second period of the rice breaking through the water surface until the fields are ultimately drained for harvest, rice vegetation above the water surface may act as double-bounce/cornerstone reflectors. The characteristic interaction between active C-band microwave signals and rice phenology is discussed in e.g. [1-3] and is considered as well established.

**Changes in manuscript:**

We completely reformulated the argument being made.

Section 5.1.1, Page 16, Line 6

“During the early phenological growth phase of rice, this observation can be attributed to specular reflection of the radar signal from the flood water surface, given that wind speeds do not significantly affect the water’s surface roughness [2]. By the time the rice stems start to break through the water surface the now elongated rice stems are known to act as double-bounce reflectors, which commonly results in an enhanced backscatter signal that can be observed until field drainage in late summer [1,3] (see ASCAT soil moisture time series in figure 5b).”

**References:**

- [1] Le Toan, T., Ribbes, F., Wang, L. F., Floury, N., Ding, K. H., Kong, J. A., ... & Kurosu, T. (1997). Rice crop mapping and monitoring using ERS-1 data based on experiment and modeling results. *IEEE Transactions on Geoscience and Remote Sensing*, 35(1), 41-56.
- [2] Nguyen, D. B., Clauss, K., Cao, S., Naeimi, V., Kuenzer, C., & Wagner, W. (2015). Mapping rice seasonality in the Mekong Delta with multi-year Envisat ASAR WSM data. *Remote Sensing*, 7(12), 15868-15893.
- [3] Nguyen, D. B., Gruber, A., & Wagner, W. (2016). Mapping rice extent and cropping scheme in the Mekong Delta using Sentinel-1A data. *Remote Sensing Letters*, 7(12), 1209-1218.
- 

**A.14. “Section 5.2 and Figure 4: Can you attribute the rainfall seasonality as another reason why satellite data doesn’t seem to detect irrigation. For SMAP, only about 2 years are included. Out of the two, 2016 is considered a wet year over the Midwest, which means there may not have been many days with differences between model and satellite data. Can you provide a figure that indicates the number of days that went into Figure 4, which could help to explain the role of rainfall seasonality.”**

**Reply:**

Here, the reviewer raises a very important point. Indeed, during ‘wet’ years we expect that the method is less skillful in detecting and quantifying irrigation events. Since figure 4 indicates the average amount of irrigation per year and for SMAP only 2 years of data are available, we created the requested plot in a normalized fashion: i.e., plotted the number of days with irrigation > 0 (according to the method) normalized by the number of years which went into the overall estimation (4 for ASCAT and AMSR-2, 2 for SMAP). The plot therefore indicates the average number of irrigation events (detected by the method) per year.

**Changes in manuscript:**

We added the new plot(s) to the supplement (Figure A3) and included a brief discussion regarding the role of rainfall seasonality in Section 5.2, Page 18, Lines 23-30:

“Rainfall seasonality is another potential reason for the underestimation in the central U.S, where the climate transitions from arid in the west to humid in the east. To investigate its impact, we plotted the average number of days per growing season where IWU > 0 (figure A3), which sums up to the number of days that went into the IWU estimates shown in figure 4. It can be seen that for SMAP based IWU , a significant number of days with irrigation

(mean count) only is detected in the arid west and south-west. For AMSR2, the mean counts are highest in California, although counts in the range of 20-30 occur in the Snake River Valley, Mississippi Flood Plain and other agricultural regions. In agreement with the passive products, mean counts for ASCAT are highest in California and south-western states. There also is a clear pattern in the Mississippi Valley and along the south-eastern states.”

---

**A.15. “Figure 5: The choice of the single point sounds a bit arbitrary. Why not, say, do an average of the pixels with irrigated area > 70% (Figure 1). That way you have some spatial representativeness in these time series comparisons.”**

**Reply:**

We understand your criticism. However, the fractional irrigated area in itself is not most relevant, as we are interested in the amount of water applied for irrigation. Specifically, we care about entangling conditions at the scale of field districts to investigate the impact of varying regional irrigation practices and crop types as well as climate conditions. Therefore, there would be no added spatial representativeness in averaging all pixels with say irrigated area > 70%, because the individual cases are far too heterogeneous.

**Changes in manuscript:**

None

## **Reviewer B:**

**“With great interest I have read this study trying to quantify irrigation amount from spatial remote sensing and land surface reanalysis. Manuscript is well written in good English and clear, results are well supported by figures, title and abstract reflect the work presented. It is relevant for HESS Readers.”**

### **Reply:**

We thank the reviewer for his positive response. Moreover, we are delighted to hear that for you the manuscript was an interesting read and that you consider it as relevant for the HESS readership.

**“I suggest that Authors do some more bibliography as I am missing some relevant work on modelling (and even assimilation) as well as mapping of irrigated areas from the introduction. I also recommend Authors to have a careful read as e.g, many acronyms are missing. It is a very interesting study, stemming on previous work from e.g. Kumar et al., 2015, but yet I am not completely convinced (and Authors will have to prove me wrong), that is why my recommendation is major review.”**

### **Reply:**

We thank the reviewer for the overall interest in our study. We have tried to include more literature (including the important suggestions you made) to enhance the discussion of modelling and data assimilation in the context of irrigation quantification. We hope that by now, we have made the necessary steps to convince you.

---

**B.1. “P.2, L11-13: “It influences the surface water and energy balance through directly increasing soil moisture, which in turn modulates the partitioning of energy between sensible and latent heat (Seneviratne et al., 2010).” I find this sentence slightly simple, is the link with the reference fully appropriate? Are Seneviratne et al., 2010 clearly mentioning irrigation or are they indicating soil moisture in general?, OK soil moisture is increased on irrigated land but water has to come from somewhere else right? Sometimes it is sourced nearby, sometimes not. I think it has to be reflected in the text.”**

### **Reply:**

We thank you for your criticism regarding the reference of Seneviratne et al. 2010. Indeed, the citation in the first sentence is a bit confusing. We meant to only reference the second part of the sentence (i.e., "... which in turn modulates the partitioning of energy between sensible and latent heat (Seneviratne et al., 2010)."). However, it reads as if the reference corresponds to the whole sentence, whereas the paper only explicitly refers to soil moisture, as already outlined by yourself. In order to eliminate potential confusion, we chose to divide the sentence into two parts.

### **Changes in manuscript:**

**Section 1, Page 2, Line 11**

“Irrigation influences the surface water and energy balance through directly increasing soil moisture. In turn, soil moisture is widely known to modulate the partitioning of energy between sensible and latent heat (Seneviratne et al., 2010).”

---

**B.2. “P.2, L.31: “To date, irrigation practices are typically not explicitly included in land surface, [...]” you are right, however some studies have emerged from a modelling point of view (e.g. work from Lawstone et al., 2015 over the US) and even data assimilation point of view (see recent work from Kumar et al., 2018 on the US NLDAS for irrigation intensity over CONUS). I believe it has to be acknowledge in your study.”**

**Reply:**

We thank you for referring to these interesting papers. Indeed, we were not aware enough of recent literature regarding the modelling and assimilation of irrigation data. To address this shortcoming, we have revised and extended the respective paragraph on irrigation modelling and data assimilation by including a discussion of both [1] and [2].

**Changes in manuscript:**

**Section 1, Page 2, Line 31 to Page 3, Line 24**

“To date, irrigation practices are typically not explicitly included in land surface, climate, or weather models. On the other hand, irrigation directly impacts land surface temperature, humidity, and soil moisture observations, and through them indirectly impact model simulations when they are being assimilated (Tuinenburg and Vries, 2017). A range of climate modelling studies employed irrigation modules on a global scale. Mainly based on a combination of static spatial maps of irrigated area and soil moisture and/or vegetation data, they tried to approximate seasonal IWU (Lobell et al., 2006; Bonfils and Lobell, 2007; Kueppers et al., 2007). However, the simulated impact of irrigation on both global and regional climate showed considerable variation across studies. With respect to a contiguous U.S. domain, Lawston et al. (2015) assessed the effects of drip, flood, and sprinkler irrigation methods during a climatically dry and wet year on land–atmosphere interactions. They used the National Aeronautics and Space Administration’s (NASA) high-resolution Land Information System (LIS) and the NASA Unified Weather Research and Forecasting Model (NU-WRF) framework both in offline and coupled simulations. In accordance with previous studies, they found that irrigation indeed cools and moistens the surface over and downwind of irrigated areas. Moreover, they found that the magnitude of this irrigation cooling effect (ICE) strongly depends on the parametrization of the respective irrigation methods. In a very recent study, KUMAR et al. (2018) conducted a multisensor, multivariate land data assimilation experiment over the CONUS by using the NASA LIS to enable the National Climate Assessment (NCA) Land Data Assimilation System (NCA-LDAS). Particularly, the use of a larger-than-normal range of soil moisture data records and snow depth data from microwave remote sensing combined with an irrigation intensity map systematically improved soil moisture and snow depth simulations.

With respect to the discrepancies in the global modelling studies, Sacks et al. (2009) argued that they can be primarily explained by systematic differences in the control of irrigation water application within the respective modules, e.g. by climate, food demand, and



economical conditions. Logically, this arguments also holds true for the modelling study by Lawston et al. (2015). Regarding the irrigation forcing used in KUMAR et al. (2018), we argue that the term "irrigation intensity" gives a false impression. Irrigation intensity in a physical sense should not be attributed to fractional irrigated area, but must rather be connected to the actual irrigation water use per unit area. In addition, fields may be either over- or under-irrigated with respect to the physically "ideal" amount. Hence, current irrigation modules are unable to consistently reflect real-world conditions and thus introduce uncertainties in modelling and data assimilation. Consequently, information on the spatio-temporal distribution and development of actual IWU is needed to improve the representation of land-atmosphere feedbacks in model simulations (Ozdogan et al., 2010a)."

#### **References:**

- [1] Lawston PM, Santanello JA Jr, Zaitchik BF, Rodell M (2015) Impact of irrigation methods on land surface model spinup and initialization of WRF forecasts. *J. Hydrometeor.* 16(3):1135–1154
- [2] Kumar, S. V., Jasinski, M., Mocko, D., Rodell, M., Borak, J., Li, B., Kato Beaudoin, H., and Peters-Lidard, C. D.: NCA-LDAS land analysis: Development and performance of a multisensor, multi-variate land data assimilation system for the National Climate Assessment, *J. Hydrometeor.*, <https://doi.org/10.1175/JHM-D-17-0125.1>, online first, 2018."
- 

**B.3. "P.3, section 1.1 on Statistics on irrigated areas and water withdrawals, I am surprised that some more recent work from e.g. Siebert et al. is not mentioned here, please see Siebert et al., 2015 and Meier et al., 2018."**

#### **Reply:**

We thank the reviewer for pointing us towards more recent literature on global irrigated area statistics. We interweaved the core messages of the two papers in section 1.1.

#### **Changes in manuscript:**

We modified Section 1.1, Page 4, Line 2 to include [1]:

"In subsequent versions the resolution was improved to 5'x5' (Siebert et al., 2005, 2007) and a new global historical irrigation data set providing time series of AEI between 1900 and 2005 was developed (Siebert et al., 2015)."

We modified Section 1.2.1, Page 5, Line 16 to include [2]:

However, there are large discrepancies between the different global data sets mainly stemming from varying definitions of irrigated areas among the data sets (i.e. area equipped for irrigation, irrigated area and cropped area) and differing reference years (i.e., the years 2000 and 2005) (Salmon et al., 2015; Meier et al., 2018)."

#### **References:**

- [1] Siebert, S., Kummu, M., Porkka, M., Döll, P., Ramankutty, N., & Scanlon, B. R. (2015). A global data set of the extent of irrigated land from 1900 to 2005. *Hydrology and Earth System Sciences*, 19(3), 1521-1545.

[2] Meier, J., Zabel, F., & Mauser, W. (2018). A global approach to estimate irrigated areas—a comparison between different data and statistics. *Hydrology and Earth System Sciences*, 22(2), 1119-1133.

---

**B.4. “P.4, L.15, please rephrase and extend or remove, it can be better introduced.”**

**Reply:**

We agree that at this specific location the introduction of remote sensing for irrigation mapping was too fuzzy. We therefore chose to move (and modify) lines 15-16 to section 1.1, which in our view establishes the connection with section 1.2 without appearing as too short.

**Changes in manuscript:**

We removed the sentence and added a new one to [Section 1.1, Page 4, Line 14](#) in order to link to Section 1.2:

“On the basis of these drawbacks, remote sensing evolved as an effective tool to potentially overcome these limitations since it provides synoptic, independent and timely information of biogeophysical variables that are either directly or indirectly related to irrigation.”

---

**B.5. “P.4, L.25, please provide acronym for USGS (anf later in the text CRU, DEM, ISBA, SURFEX...all acronyms have to be explained).”**

**Reply:**

We thank the reviewer for pointing out that several acronyms were left unexplained. In the revised manuscript version, all acronyms are now correctly introduced.

**Changes in manuscript:**

We have now introduced the missing explanations for each of the following acronyms:

- USGS : United States Geological Survey
- CRU : Climate Research Unit
- DEM : Digital Elevation Model
- ISBA : Interaction Sol Biosphère Atmosphère
- SURFEX : Surface Externalisée

**References:**

Explanations for each acronym were provided within the respective literature.

---

**B.6. To organize our replies, we split this comment into three sections:**

- a) “P.6, L.11-14, this sentence caught my interest, assuming that microwave remote sensing is sensitive to the very first cm of soil, at least at X- and C-band, could you detect all irrigation types? Is dripping/micro-irrigation leading to a sufficient change in soil moisture to be noticed from space?
- b) What about vegetation masking the ground? We all have in mind pictures of irrigated (fully developed) corn, can remote sensing see through that? Although it is mentioned in 5.1.3 maybe it could ruled out C-band? At least for certain period of vegetation cycle.

- c) **By the way, why not considering SMOS L-band mission, my understanding is that it should be more sensitive to soil moisture than the sensors you use (?). SMAP is used but in combination with SMOS (I am aware that combined products exist) it would lead to a longer period being investigated.”**

**Reply:**

a.) This is a crucial question. In the manuscript, we tried to stress the fact that different irrigation techniques are expected to critically impact the sensitivity of microwave observations. For instance, see Section 2.1, Page 7, Lines 31-32 expanding to Page 8, Line 1: “It is likely that the sensitivity of satellite soil moisture retrievals to irrigation increases when the irrigation application efficiency of a particular irrigation system or technique deteriorates. Therefore, we expect higher sensitivity towards gravity- (e.g. flood and furrow irrigation), and lower sensitivities towards sprinkler- and micro-irrigation systems.” This dependency should also vary between L- and C-band, however we argue that the ability to sense “the very first centimeter of soil” is too pessimistic. With respect to irrigation, we are not aware of any observationally driven studies investigating this issue in-depth, so we don’t know for sure what is the actual case. However, in [1], drip, sprinkler, and flood irrigation parameterizations are assessed in a modelling domain. Regarding your question, we think that the most important points made in this study are:

- i) Even in developed countries such as the U.S., micro-irrigation is very rare (e.g., 1% of farmers in the Central Plains use it to an unknown extent), since it is more cost and labour intensive. Therefore, it is very likely that it only accounts for a very small portion of the overall water usage.
- ii) The top-panel in Figure 2 shows “monthly, domain-averaged differences from Control in top-layer soil moisture SM” for each irrigation method. The authors state that: “As anticipated, Drip exhibits zero changes to soil moisture content because of the nature of the algorithm, as additional water is immediately used for transpiration.” In real-world examples, this budget-closure likely won’t be the case, but certainly very close to it. Here, one has to differentiate between surface- and subsurface-drip-irrigation. Sub-surface irrigation at the plants root zone has the goal of not even wetting the soil, so the impact on soil moisture is negligible. For surface drip-irrigation, the soil wetting effect will probably be very minor.
- iii) They also state that although soil moisture is not impacted directly by drip irrigation, the method does have an effect on soil temperature and hence on latent heat flux and surface temperature. So although soil moisture is not directly affected by drip irrigation in the model output, there is considerable impact on the energy- and water-cycle. However, this is not the main subject of our study.

Based on these observations, we argue that the impact of micro-irrigation (such as drip irrigation) on space-borne soil moisture observations will likely be below the retrieval error, if measurable at all.

**b.)** This is another important point. The reality is that we are not completely sure what is the case. Specifically at the start of the study, we had problems with the active ASCAT soil moisture product over the Corn Belt (see [2]), which according to USGS accounts for the majority of U.S. corn production. We figure that during the latter stages of crop development, when corn reaches significant heights (which in the end can potentially be in the order of 2.5-3m), the microwave signal will still partly reflect soil moisture. As outlined in the reply to comment A.1., ASCAT soil moisture was repeatedly shown to perform well over densely vegetated areas. However, we also expect that volume scattering effects (in the active sensing case) and vegetation water content (in the passive sensing case) might increasingly affect the overall signal. In the end, this is more related to the vegetation correction of each respective retrieval algorithm and hence is out of the scope of this study.

**c.)** Concerning the use of SMOS soil moisture, we also kindly refer to our replies to comment A.1. Concerning the use of a combined SMAP-SMOS soil moisture product, we agree that this could be a very valuable addition, but advocate that before using multi-sensor data (e.g., ESA CCI soil moisture, SMAP-SMOS soil moisture data records), we should assess the specific sensitivities of each sensor with respect to irrigation quantification.

**Changes in manuscript:**

None

**References:**

- [1] Lawston, P. M., Santanello Jr, J. A., Zaitchik, B. F., & Rodell, M. (2015). Impact of irrigation methods on land surface model spinup and initialization of WRF forecasts. *Journal of Hydrometeorology*, 16(3), 1135-1154.
- [2] Zaussinger, F., Dorigo, W., & Gruber, A. (2017, April). Estimating irrigated areas from satellite and model soil moisture data over the contiguous US. In EGU General Assembly Conference Abstracts (Vol. 19, p. 7713).

---

**B.7. "P.6, L.27, please add reference for SURFEX (Masson et al., 2013)."**

**Reply:**

Thank you for pointing out the missing reference, we have added your suggestion [1].

**Changes in manuscript:**

**Section 1.2.2, Page 7, Lines 32-35:**

"Escorihuela and Quintana-Seguí (2016) compared three global satellite soil moisture products (ASCAT, AMSR-2 and SMOS) with model soil moisture estimates from the Surface Externalisée (SURFEX) model (Masson et al., 2013) (forced with meteorological data) in the Mediterranean."

## **References:**

[1] Masson, V., Le Moigne, P., Martin, E., Faroux, S., Alias, A., Alkama, R., ... & Brousseau, P. (2013). The SURFEXv7. 2 land and ocean surface platform for coupled or offline simulation of earth surface variables and fluxes. *Geoscientific Model Development*, 6, 929-960.

---

**B.8. “P.6, L.32, “[...] that SMAP soil moisture carries a clear irrigation signal from rice irrigation [...]”, could you please specify irrigation type, flooding (as it is likely to be water seeded)? Did SMAP sees open-water there?”**

## **Reply:**

As this statement directly refers to the study conducted by Lawston et. al., 2017 (who used the SMAP product sampled to a 9 km grid), we cannot make a definite statement. However, since part of our time series analysis is based on the same study region (Sacramento Valley, California), we are confident that SMAP sensed open water during a certain period of time.

## **Changes in manuscript:**

None

---

**B.9. “P.11, L.4, didn’t you say earlier that this map was not reliable? Please clarify.”**

## **Reply:**

We agree that in the current state, the discussion of the ESA CCI land cover product is misleading. To clarify, this product proves to provide a very reliable indicator for agricultural land cover in general, but shows a low performance in further classifying irrigated and non-irrigated agriculture. In addition, it is subject to misclassification in other parts of the world (see [1]). Since we are only interested in mask for agricultural land in general, we can use this map. As you point out, in Section 1.2.1, Page 5, Lines 2-4, we make the case that “...the irrigated class is likely to be considered unreliable...”.

## **Changes in manuscript:**

In order to eradicate potential confusion, we propose to clarify our choice in [Section 3.3, Page 12, Line 4](#): “Despite the drawbacks discussed in section 1.2, the ESA CCI Land Cover data set (Bontemps et al., 2013) was used to create a cropland mask for the CONUS, because the classification of overall agricultural land cover (i.e., irrigated and rainfed lands) proved to be accurate.”

In addition, we modified [Section 1.2.1, Page 5, Lines 2-4](#). It now reads as follows: “It distinguishes irrigated and non-irrigated cropland for 2000, 2005 and 2010. However, we argue that over the contiguous United States (CONUS) the irrigated class is likely to be considered unreliable, as apparently all irrigated lands are wrongly attributed to the non-irrigated agriculture class.”

---

**B.10. “Section 3.4, then considering SMOS would make it possible investigating longer period of time.”**

**Reply:**

Since the first reviewer also commented on SMOS, we already addressed the topic in the replies to the first reviewer. Therefore, we kindly refer to our reply on comment A.1.

---

**B.11. “P.11, L.18-23, please see work from Kumar et al., 2015 on the scaling issue.”**

**Reply:**

The scaling issue was addressed in comment A.2. of the other reviewer. We kindly refer to our reply above.

---

**B.12. To organize our replies, we split this comment into five sections:**

- a) “P.12, sections 4.1 to 4.3, so a big assumption is that the mismatch between model and satellite soil moisture is irrigation, so the forcing is assumed to be perfect and we know that is not the case.
- b) I am also curious on the possible mismatch between what land cover the satellite is really sensing and what MERRA2 has for land cover.
- c) The same is true for soil texture, porosity and all ancillary data...could it lead to spurious irrigations/non-irrigation?
- d) And what about temporal mismatch? Do you consider the satellite soil moisture revisit time enough for such study? If it rains after the satellite has passed (but maybe it a silly thought as you consider rain free period -according to the forcing)? Please comment on this issue.
- e) You should also assess your method in areas where crops are rain-fed only to see what signal is detected when we know that no irrigation occurs (see 5.1.3!)”

**Reply:**

- a) Yes, this is the main assumption. By applying the mean-stdv scaling, we implicitly also correct for deviations in spatial representativeness etc., as discussed in the reply to comment A.03. Of course, the forcing is not perfect. Since rainfall is arguably the most important model forcing over the land surface, we use information from an additional CPC precipitation data set at 0.25° resolution. This basically allows us to have a 4x better spatial resolution when evaluating whether or not an irrigation event is present compared to the native rainfall forcing in MERRA-2. However, we do not gain more resolution with respect to soil moisture and ultimately irrigation estimation.
- b) We agree that this is an important point. In addition, while the model land cover usually remains static/semi-static, the satellite microwave observations are constantly sensitive to changes in land cover. However, such an evaluation would require a reliable land cover reference data set and would imply an actual land cover validation of the MERRA2 land surface model, which is beyond the scope of this study. Maybe this issue can be addressed in future studies.

- c) Mismatches in ancillary data such as soil parameters would imply a bias in the soil moisture dynamic range of the model. Since we scale the satellite data to this dynamic range, we implicitly account for such mismatches.
- d) The satellite revisit time arguably has a big impact. In [1], our co-authors conducted a synthetic experiment to analyze the impact of revisit time (among other factors such as retrieval error and climate) on irrigation quantification. They found that the performance of their method significantly deteriorates for revisit times > 3 days. Concerning our study, as outlined in Section 4.2, Page 13, Lines 10-14, this is an intrinsic limitation of the method: “If an irrigation event is detected during an observation gap of > 4 days, we check if there has been a significant increase in the model soil moisture (e.g. due to rainfall) within that period. When more than one significantly positive model slopes (or precipitation events) occur during the gap-period, we cannot say for sure if the observed increase in soil moisture was due to irrigation or precipitation and therefore conservatively disregard the potential irrigation event.”
- e) In each of the four focus regions, parts of the “non-irrigated” reference pixels are rainfed crops (see section 5.3), so we think that this is already being taken into account. Of course, we had to make a trade-off between geographical proximity (very similar climate, crops, etc...) and a large fraction of rainfed cropland.

**Changes in manuscript:**

We tried to address comments a) - c) by extending and re-writing the discussion on spurious irrigation events in [section 4.3, page 15](#):

“Potential errors may arise when the model forcing misses or creates false rainfall events. In addition, because of differences in timing of the estimates and differences in represented soil depth between remotely sensed and modelled soil moisture, their response to precipitation events may differ as well. This can lead to spurious irrigation events when irrigation is estimated at days with rainfall. Therefore, we use information from an additional CPC precipitation data set at 0.25° resolution, thus providing approximately 4x higher spatial resolution than the rainfall product used to force MERRA-2 (see section 3.2). This allows us to make a more educated guess when evaluating if the observations and/or model estimates are affected by rainfall.

Furthermore, if a potential irrigation signal coincides with preceding rainfall we assume that irrigation is unlikely and disregard the event. In some extreme cases, capillary rise from deeper soil layers or run-on can wet the top soil. Theoretically, these conditions are reflected by the satellite soil moisture retrievals, but absent in the model soil moisture simulations (i.e. if such effects are not accounted for in the soil hydrology formulation of the LSM (McColl et al., 2017)). However, at the large spatial scales represented by the employed satellite (approximately 25 km) and model soil moisture products (approximately 50 km), very few pixels are expected to show positive  $\Delta\Theta_{sat}$  or  $\Delta\Theta_{mod}$  in the absence of precipitation or irrigation.



Another impact concerns mismatches between the ancillary data used to force the model and parametrize the respective satellite soil moisture retrieval algorithms, such as land cover and soil parameters. By rescaling to the model dynamic soil moisture range, we implicitly account for mismatches in soil parameters. However, addressing potential mismatches in land cover was out of the scope of this paper and thus represent an intrinsic limitation of the method.”

**References:**

[1] Brocca, L., Tarpanelli, A., Filippucci, P., Dorigo, W., Zaussinger, F., Gruber, A., & Fernández-Prieto, D. (2018). How much water is used for irrigation? A new approach exploiting coarse resolution satellite soil moisture products. *International Journal of Applied Earth Observation and Geoinformation*, 73, 752-766.

---

**B.13.** “P.18, L.7, typo (?) “due to””

**Reply:**

We thank the reviewer for pointing out the typo and have corrected it.

**Changes in manuscript:**

Page 18, Line 7

“First, due to the abundant rainfall during the growing season only supplemental irrigation is applied in this area.”

---

**B.14.** “P.21, L.7-8, “Consequently, microwave soil moisture retrievals are expected to be most sensitive to flood irrigation, followed by sprinkler- and micro-irrigation [...]” are microwaves less sensitive to micro-irrigation or not at all?”

**Reply:**

Please see our reply to your comment B.6.(a).

---

**B.15.** “Pleas reshape figure 6 as text is hardly readable (and label panels as much as possible for sack of clarity”

**Reply:**

We thank the reviewer for the suggestions for improving the readability of figure 6 and have reorganized it.

**Changes in manuscript:**

Page 37, Figure 6: Page 37, Figure 6

We have increased the font sizes and deleted the county labels for improved readability.

# Estimating irrigation water use over the contiguous United States by combining satellite and reanalysis soil moisture data

Felix Zaussinger<sup>1</sup>, Wouter Dorigo<sup>1</sup>, Alexander Gruber<sup>1,2</sup>, Angelica Tarpanelli<sup>3</sup>, Paolo Filippucci<sup>3</sup>, and Luca Brocca<sup>3</sup>

<sup>1</sup>CLIMERS - Research Group Climate and Environmental Remote Sensing, Department of Geodesy and Geoinformation, TU Wien, Vienna, Austria

<sup>2</sup>Department of Earth and Environmental Sciences, KU Leuven, Heverlee, Belgium

<sup>3</sup>Research Institute for Geo-Hydrological Protection, National Research Council, Perugia, Italy

**Correspondence:** Felix Zaussinger (felix.zaussinger@geo.tuwien.ac.at) and Wouter Dorigo (wouter.dorigo@geo.tuwien.ac.at)

**Abstract.** Effective agricultural water management requires accurate and timely information on the availability and use of irrigation water. However, most existing information on irrigation water use (IWU) lacks the objectivity and spatio-temporal representativeness needed for operational water management and meaningful characterisation of land-climate interactions. Although optical remote sensing has been used to map the area affected by irrigation, it does not physically allow for the estimation of the actual amount of irrigation water applied. On the other hand, microwave observations of the moisture content in the top soil layer are directly influenced by agricultural irrigation practices, and thus potentially allow for the quantitative estimation of IWU. In this study, we combine surface soil moisture retrievals from the spaceborne SMAP, AMSR2, and ASCAT microwave sensors with modelled soil moisture from MERRA-2 reanalysis to derive monthly IWU dynamics over the contiguous United States (CONUS) for the period 2013-2016. The methodology is driven by the assumption that the hydrology formulation of the MERRA-2 model does not account for irrigation, while the remotely sensed soil moisture retrievals do contain an irrigation signal. For many CONUS irrigation hot spots, the estimated spatial irrigation patterns show good agreement with a reference data set on irrigated areas. Moreover, in intensively irrigated areas, the temporal dynamics of observed IWU is meaningful with respect to ancillary data on local irrigation practices. State-aggregated mean IWU volumes derived from the combination of SMAP and MERRA-2 soil moisture show a good correlation with statistically reported state-level irrigation water withdrawals but systematically underestimate them. We argue that this discrepancy can be mainly attributed to the coarse spatial resolution of the employed satellite soil moisture retrievals, which fails to resolve local irrigation practices. Consequently, higher resolution soil moisture data are needed to further enhance the accuracy of IWU mapping.

## 1 Introduction

The agricultural sector uses over 70 % of global freshwater withdrawals for irrigation (Shiklomanov, 2000; Foley et al., 2011). As a result of world population increase and rising living standards water will be a major constraint for agriculture in the coming decades. In addition, climate change will likely have a profound impact on irrigation demand throughout the world.

5 The projected increase in global mean temperature and changing precipitation patterns are expected to decrease natural water availability in already water-scarce regions of the world (Vörösmarty et al., 2000; Rockström et al., 2012; Kummu et al., 2016). For instance, Döll (2002) showed that around 2/3rd of the areas that were irrigated in 1995 will require more irrigation water by 2070. Moreover, predictions show that the hydrological cycle will intensify. Hence, drought and flood events are expected to occur both more frequently and severely, which further impairs water availability for agriculture (Allan and Soden, 2008).

10

On the other hand, irrigation itself is an important anthropogenic climate forcing (Sacks et al., 2009). It influences the surface water and energy balance through directly increasing soil moisture, ~~which in turn modulates~~. In turn, soil moisture is widely known to modulate the partitioning of energy between sensible and latent heat (Seneviratne et al., 2010). Subsequently, irrigation cools the land surface on local to regional scales through increasing evapotranspiration (ET), whereas the increased

15 availability of atmospheric water ~~vapor~~ vapour can enhance cloud cover and precipitation (Boucher et al., 2004; Lobell et al., 2006; Sacks et al., 2009). Researchers agree that irrigation may have masked the full warming signal caused by greenhouse gas emissions (Bonfils and Lobell, 2007; Kueppers et al., 2007). As a past expansion of irrigated area and an overall increase in irrigation intensity may have significantly affected surface temperature observations, it is crucial to include irrigation impacts both in understanding historical climate and modeling ~~modelling~~ future climate trends (Lobell et al., 2006). Assuming a similar

20 expansion of irrigation as in recent decades, some regions may actually benefit from this irrigation cooling effect. As outlined in Ozdogan et al. (2006), ET and in turn irrigation water requirements can decrease within agricultural micro-climates. However, non-linear repercussions on temperature extremes can be expected when the required water supply cannot be met (Thiery et al., 2017) and (semi-)arid regions are generally expected to be adversely affected by water scarcity (Kueppers et al., 2007). As a consequence, especially in water-scarce regions, government agencies and water managers are challenged to increase water

25 use efficiency, optimise the distribution of water among farms, and detect illegal groundwater pumping activities (Siebert et al., 2010; Taylor et al., 2012). For example, as a consequence of prolonged winter precipitation deficits and positive temperature anomalies from 2012-2017 a record breaking drought peaking in 2015 affected the California Central Valley. While farmers tried to compensate the 2015 surface water shortage by pumping more groundwater, a net water shortage of over 3 km<sup>3</sup> resulted in the fallowing of approximately 230 000 ha of land (Howitt, 2015).

30

To date, irrigation practices are typically not explicitly included in land surface, climate, or weather models. On the other hand, irrigation directly impacts land surface temperature, humidity, and soil moisture observations, and through them indirectly impact model simulations when they are being assimilated (Tuinenburg and Vries, 2017). ~~In recent years, a~~ A range of climate modelling studies employed irrigation modules ~~, which were mainly on a global scale. Mainly~~ based on a combi-

nation of static spatial maps of irrigated area and soil moisture and/or vegetation data, they tried to approximate seasonal IWU (Lobell et al., 2006; Bonfils and Lobell, 2007; Kueppers et al., 2007). However, the simulated impact of irrigation on both global and regional climate showed considerable variation across studies. With respect to a contiguous U.S. domain, Lawston et al. (2015) assessed the effects of drip, flood, and sprinkler irrigation methods during a climatically dry and wet year on land-atmosphere interactions. They used the National Aeronautics and Space Administration's (NASA) high-resolution Land Information System (LIS) and the NASA Unified Weather Research and Forecasting Model framework both in offline and coupled simulations. In accordance with previous studies, they found that irrigation indeed cools and moistens the surface over and downwind of irrigated areas. Moreover, they found that the magnitude of this irrigation cooling effect (ICE) strongly depends on the parametrization of the respective irrigation methods. In a very recent study, Kumar et al. (2018) conducted a multi-sensor, multivariate land data assimilation experiment over the CONUS by using the NASA LIS to enable the National Climate Assessment Land Data Assimilation System. Particularly, the use of a larger-than-normal range of soil moisture data records and snow depth data from microwave remote sensing combined with an irrigation intensity map systematically improved soil moisture and snow depth simulations.

With respect to the discrepancies in the global modelling studies, Sacks et al. (2009) argued that ~~this discrepancy is they can be~~ primarily explained by systematic differences in the control of irrigation water application within the respective modules, e.g. by climate, food demand, and economical conditions. ~~Also, Logically, this arguments also holds true for the modelling study by Lawston et al. (2015).~~ Regarding the irrigation forcing used in Kumar et al. (2018), we argue that the term "irrigation intensity" gives a false impression. Irrigation intensity in a physical sense should not be attributed to fractional irrigated area, but must rather be connected to the actual irrigation water use per unit area. In addition, fields may be either over- or under-irrigated with respect to the physically ~~ideal~~"ideal" amount. Hence, current irrigation modules are unable to consistently reflect real-world conditions and thus introduce uncertainties in ~~the model simulations~~modelling and data assimilation. Consequently, information on the spatio-temporal distribution and development of actual IWU is needed to improve the representation of land-atmosphere feedbacks in model simulations (Ozdogan et al., 2010a).

## 25 **1.1 Statistics on irrigated areas and water withdrawals**

Available information on irrigated areas and particularly irrigation water use lacks objectivity, spatial consistency and temporal resolution needed for large-scale hydrological assessments and ~~modeling~~modelling (Deines et al., 2017). On local to regional scales, some irrigation districts conduct regular surveys, but often the data are not publicly available, lack geo-referencing and are difficult to compare between regions due to different sampling techniques. The elementary source of large-scale irrigation data are national and sub-national statistical units, which in most countries routinely collect information on irrigated area and/or irrigation water withdrawals. Data are usually represented as area equipped for irrigation (AEI), and in some cases also reflect the area actually irrigated (AAI) in the respective year of the census (Siebert et al., 2005)). The Global Map of Irrigation Areas (GMIA) was the first global-scale geospatial irrigated area data set (Döll, 2002; Döll and Siebert, 2002) based on such statistics. GMIA combines sub-national irrigation data from various sources (FAO, UN, World Bank, Agriculture Departments)

and geospatial information on the location and extent of irrigation schemes (point-, polygon- and raster data, land cover maps, and satellite imagery) to map AEI and AAI at 0.5° resolution around the year 2000. In subsequent versions the resolution was improved to 5'x5' (Siebert et al., 2005, 2007) [and a new global historical irrigation data set providing time series of AEI between 1900 and 2005 was developed \(Siebert et al., 2015\)](#). However, the large variability in the quality of the underlying

5 statistical inventory data is propagated into the uncertainty of the final spatial map (Siebert et al., 2005).

In summary, the main limitations of statistical inventories and derived products are:

1. The quality of the data varies significantly among countries (Siebert et al., 2010). While for instance the United States agricultural census is considered to have high quality, many developing countries lack the resources for comprehensive reporting.
- 5 2. National statistics are usually only valid for single years and depend on the individual compilation cycle of each country (e.g. every 5 years in case of the US).
3. Irrigated area estimates usually reflect areas equipped for irrigation, rather than areas actually irrigated. Depending on climatic and market conditions, farmers may decide to only cultivate and irrigate a portion of their fields.
4. Irrigation volume estimates reflect irrigation water withdrawals rather than actual irrigation water use (e.g. if rainfall is sufficient, already withdrawn spare water is stored in reservoirs instead of being irrigated)
- 10 5. Naturally, survey-based statistics are only based on a sample of farms, which may not be representative.
6. Conventional methods are unable to reflect illegally withdrawn water used for irrigation (Roseta-Palma et al., 2014; Saffi and Cheddadi, 2010).

## 1.2 Remote sensing for irrigation mapping

15 ~~Remote sensing offers the potential to overcome the limitations of statistical inventories by providing synoptic~~ On the basis of these drawbacks, remote sensing evolved as an effective tool to potentially overcome these limitations since it provides synoptic, independent and timely information of biogeophysical variables that are either directly or indirectly related to irrigation.

## 1.2 Remote sensing for irrigation mapping

### 20 1.2.1 Optical and thermal remote sensing

Data acquired by optical sensors (AVHRR, MODIS, Landsat) have been extensively used to identify irrigated areas on local-, regional- and global scales. Vegetation indices have been identified as effective proxies for irrigation practices, because irrigated and non-irrigated cropland show different spectral responses during the peak growing season (Ozdogan et al., 2010b). A wide range of studies used vegetation indices to map annual irrigated areas and their changes through time, sometimes in  
25 combination with statistical inventory data.

Only few global land use-land cover (LULC) maps based on optical remote sensing separate irrigated from rainfed croplands. For example, the USGS-United States Geological Survey (USGS) Global Land Cover Characteristics (GLCC) data set was derived from 1 km Advanced Very High Resolution Radiometer (AVHRR) sensor data and identified four types of irrigated croplands in the year 1992 (Loveland et al., 2000). However, the classification algorithms used were not tailored to  
30

irrigated area mapping, thus resulting in low classification accuracies. Large discrepancies were found between USGS GLCC and country level reports of irrigated area, originating from both the uncertainties of the inventory data and technical limitations of the remote sensing data sets (Vörösmarty et al., 2000). Through a combination of unsupervised clustering and expert knowledge, the European Space Agency (ESA) Climate Change Initiative (CCI) has produced global land cover product at 300 m resolution using Medium Resolution Imaging Spectrometer (MERIS) data (Bontemps et al., 2013). It distinguishes irrigated and non-irrigated cropland for 2000, 2005 and ~~2010, but the 2010~~. However, we argue that over the CONUS the irrigated class is likely to be considered unreliable, as ~~for instance no irrigated areas were mapped within the contiguous United States (CONUS)~~ apparently all irrigated lands are wrongly attributed to the non-irrigated agriculture class.

Other studies used approaches specifically tailored to irrigated area mapping. For instance, the global data set of monthly irrigated and rainfed crop areas around the year 2000 (MIRCA2000) provides irrigated and rainfed areas for 26 crop classes for each month of the year at 5' resolution (Portmann et al., 2010). For this purpose, agricultural census statistics, national reports, databases, a map of crop specific annual harvested area, a cropland extent map, the GMIA, crop calendars and ancillary information on climate and topography were combined. Using quantitative spectral matching techniques on NDVI time series from multiple sensors (AVHRR, SPOT-1, MODIS, Landsat 7 and JERS-1 SAR) in combination with climate (monthly precipitation and temperature data from ~~CRU~~the Climate Research Unit) and ancillary data (GTOPO30 1 km ~~DEM~~digital elevation model, global tree cover), the International Water Management Institute (IMWI) produced a Global Irrigated Area Map (GIAM) at 1 km resolution around the year 2000 (Thenkabail et al., 2009). More recently, Salmon et al. (2015) created a global map of rain-fed, irrigated and paddy croplands (GRIPC) around the year 2005 at 500 m spatial resolution using supervised classification of remote sensing, climate, and agricultural inventory data. However, there are large discrepancies between the different global data sets (~~Salmon et al., 2015~~), mainly stemming from varying definitions of irrigated areas among the data sets (i.e. area equipped for irrigation, irrigated area and cropped area) and differing reference years (i.e., the years 2000 and 2005) (Salmon et al., 2015; Meier et al., 2018). Moreover, three of the four existing global maps (GMIA, MIRCA2000 and GRIPC) rely on agricultural inventory data for the classification of irrigated areas, which is subject to major limitations concerning quality and accuracy. In addition, the maps are limited to single years (GMIA, GIAM, GRIPC), or single months within a single year (MIRCA2000), thus not being able to address the high inter-annual variability of irrigated areas, which is mainly governed by climate and market conditions (Deines et al., 2017).

On a continental scale, the MODIS Irrigated Agriculture data set for the conterminous United States (MIrAD-US) was created by assimilating county level irrigation statistics with MODIS-derived seasonal peak Normalised Difference Vegetation Index (NDVI) to spatially identify irrigated and non-irrigated lands at 250 m resolution (Ozdogan and Gutman, 2008; Pervez et al., 2008; Pervez and Brown, 2010). A significant drawback is that the map compilation is tied to the same 5-year cycle of the United States Department of Agriculture (USDA) Census of Agriculture. Ambika et al. (2016) mapped irrigated areas from 2000–2015 at 250 m resolution over India by using 250 m MODIS seasonal peak NDVI data and 56 m LULC data. Teluguntla et al. (2017) used spectral matching techniques and automated cropland classification algorithms to infer cropland extent, ir-



rigated versus rainfed croplands, and cropping intensities over Australia. The latter two products allow to study inter-annual variability of irrigated areas (Ambika et al., 2016).

5 On a regional scale, higher resolution Landsat imagery was adopted by a range of studies. Ozdogan et al. (2006) used 30 m Landsat imagery to map changes in annual irrigated area from 1993 to 2002 in southeastern Turkey based on NDVI thresholding approaches and compared them with estimates of irrigation water requirements inferred from potential evapotranspiration. In a recent study, Deines et al. (2017) produced annual irrigation maps for 1999-2016 for a region in the High Plains Aquifer (United States) at 30 m resolution. Pun et al. (2017) used a combination of surface energy balance partitioning and vegetation indices to classify irrigated and non-irrigated croplands at 30 m resolution in Nebraska.

10

Thermal remote sensing has been widely used to map irrigation water based on estimating potential evaporation from surface energy heat fluxes and the application of specific crop factors (Rosas et al., 2017). A well-known technique is the Surface Energy Balance Algorithm for Land, which estimates variables of the hydrological cycle based on remotely sensed surface energy balance components (Bastiaanssen et al., 1998). In contrast, Hain et al. (2015) developed a novel method for inferring regions where non-precipitation inputs (e.g., irrigation) significantly impact terrestrial latent heat flux (LE). They compared modelled bottom-up LE (i.e., without irrigation) and top-down LE drawn from observations of diurnal land surface temperature changes which are connected to changes in the land surface moisture status and therefore irrigation. However, these methods are only able to provide estimates on irrigation water requirements (i.e. what the amount of water a plant would ideally need), as opposed to actually irrigated water, as in practice fields are often ~~over- or~~ under-irrigated.

### 20 1.2.2 Microwave remote sensing

Microwave observations are widely used to estimate soil moisture (Entekhabi et al., 2010; Wagner et al., 2013; Dorigo et al., 2017). Major advantages of microwave observations are their all-weather capability and the intrinsic capacity to sense a geophysical variable which is directly and physically linked to irrigation.

25 The first study to investigate the utility of satellite soil moisture retrievals for irrigation mapping was carried out by Kumar et al. (2015). They used soil moisture retrievals from ASCAT, AMSR-E, SMOS and Windsat, and the ESA CCI multi-satellite surface soil moisture product in combination with soil moisture estimates from the Noah LSM to map irrigated areas in the CONUS. Their key assumption was that irrigation is not included in the formulation of LSM, whereas satellite-derived soil moisture is expected to reflect the changes in soil moisture induced by irrigation. Based on synthetic data, they were able to  
30 detect differences between the probability density functions of satellite and modelled soil moisture. However, the satellite data showed only few systematic differences that could be reliably related to irrigation practices.

Qiu et al. (2016) compared trends from 1996–2010 in China of ESA CCI, ERA Interim/Land reanalysis, and in-situ soil moisture, as well as precipitation. They observed significant discrepancies between precipitation and satellite soil moisture trends

over irrigated areas, which they ascribed to irrigation. Escorihuela and Quintana-Seguí (2016) compared three global satellite soil moisture products (ASCAT, AMSR-2 and SMOS) with model soil moisture estimates from the ~~ISBA-scheme within SURFEX~~ Surface Externalisée (SURFEX) model (Masson et al., 2013) (forced with meteorological data) in the Mediterranean. Only a downscaled version of SMOS (SMOScat) showed significantly lower correlations over irrigated areas. The authors argued that primarily due to the coarse spatial resolution of the native soil moisture retrievals the other products were not able to resolve the irrigation signal from the soil moisture signal from the surrounding dry-land area. Very recently Lawston et al. (2017) investigated the potential of the new SMAP enhanced 9 km SM product to identify irrigation signals in three semi-arid regions in the western United States. Results showed that SMAP soil moisture carries a clear irrigation signal from rice irrigation in the Sacramento Valley (California), while the signals were less obvious in the other two regions (Columbia River Basin, Washington and Colorado).

### 1.3 Objective of this study

Despite the large number of studies using remote sensing approaches to map irrigated area and irrigation water requirements at various spatial and temporal scales, none of these approaches has attempted to derive actual irrigation water use. To bridge this gap, we propose a new method for estimating IWU from a combination of remotely sensed and modelled reanalysis soil moisture data. The approach is based on the hypothesis that neither the structure nor the forcing of the model data accounts for artificial water supply, while the microwave soil moisture retrievals do (Kumar et al., 2015; Escorihuela and Quintana-Seguí, 2016). The method is implemented over the ~~contiguous United States~~ CONUS by using three state-of-the-art microwave soil moisture products (i.e. based on SMAP, AMSR2 and ASCAT) in combination with MERRA-2 reanalysis soil moisture. By using passive L-band and both active and passive C-band soil moisture data, we aim to assess the impact of the microwave observation frequency and the sensing technique with respect to irrigation quantification. For this reason we only used one dataset per category.

The paper is organised as follows: section 2 provides a general overview of the irrigation landscape in the CONUS. Section 3 covers the utilised satellite-, model- and ancillary data sets and the preprocessing involved. The theoretical and practical aspects of the new methodology to estimate IWU are discussed in section 4. Results are shown and discussed with respect to official reference irrigation data in section 5. Section 6 conclude the study and gives an outlook ~~for-on~~ follow-on research.

## 2 Study area

### 2.1 Irrigation practices in the contiguous United States(~~CONUS~~)

The amount of water needed by a certain crop for optimal growth mainly depends on three factors: crop type, soil, and climate. Irrigation water need is given by the difference between these requirements for optimal crop growth and effective rainfall. In

the largely semi-humid climate of the eastern United States, irrigation is supplemental, which means that irrigation is applied to mostly rain-fed crops during times of insufficient rainfall to achieve higher yields than under rain-fed conditions alone. In contrast, the predominantly semi-arid climate of the western US makes artificial water supply a necessity, thus requiring full irrigation.

5

The 2013 Farm and Ranch Irrigation Survey (FRIS) of the National Agricultural Statistics Service (NASS) of the USDA (USDA, 2013) provides selected irrigation data from surveys conducted at approximately 35000 farms using irrigation across the US (USDA, 2013). It reports state-level data of both irrigated area and irrigation water withdrawals (IWW) subdivided by specific crop type, water source and irrigation technique. In addition, these estimates are given for crops cultivated outdoors  
10 („in the open“and indoors („under protection“, e.g. horticultural crops grown in greenhouses). Figure 1 shows per state the irrigated area and irrigation water withdrawals limited to crops grown outdoors, as well as irrigation application rates during the 2013 growing season provided by FRIS.

It is likely that the sensitivity of satellite soil moisture retrievals to irrigation increases when the irrigation application  
15 efficiency of a particular irrigation system or technique deteriorates. Therefore, we expect higher sensitivity towards gravity- (e.g. flood and furrow irrigation), and lower sensitivities towards sprinkler- and micro-irrigation systems. Fig. A1 shows a distinct decline in irrigation rates per area from the semi-arid west to the more humid east. The state of Arizona has the highest irrigation rate per area, followed by California and Nevada. Gravity flow systems show the highest rates in California and Arizona, but also depict large values along the Mississippi Delta. This can mainly be attributed to the cultivation of rice which  
20 is primarily grown in these regions and is either flood or furrow irrigated. Finally, micro-irrigation systems are largely limited to the western half of the US.

## 2.2 Focus areas

In addition to the continental-scale analysis, we chose four irrigation hot spots characterised by different climates and irrigation practices within the CONUS (Fig. 2) to comprehensively assess the spatio-temporal dynamics of irrigation. These regions are:  
25 the Sacramento Valley and San Joaquin Valley in the California Central Valley; the Snake River Plain, Idaho; the High Plains, Nebraska; and part of the Mississippi Flood Plain located within the state of Mississippi. For each focus area, we conducted a time series analysis at local scale (Sect. 5.3), as well as a cross comparison with reference data on irrigated area (Sect. 5.5) and irrigation water withdrawals (Sect. 5.4).

### 2.2.1 Central Valley, California

30 Traditionally, the California Central Valley accounts for the highest irrigation water withdrawals across the CONUS. Its northern part is characterised by a Mediterranean climate with hot, dry summers, whereas its southern half is defined by both hot and cold semi-arid climates (Kottek et al., 2006). As a result, crop production requires full irrigation. We selected two areas within the Central Valley for the time series analysis: the southern San Joaquin Valley, where several different crop types are

cultivated using sprinkler-, furrow- and micro-irrigation-systems, and the northern Sacramento Valley where flood irrigation for rice is prevalent and which was also investigated by Lawston et al. (2017). Rice production in California is the second largest in the US (NASS, 2012) and relies on large amounts of irrigation water, which is usually supplied by winter snow melt. In the Sacramento Valley, which accounts for 95 % of California's rice yield, rice is typically water-seeded (Linguist et al., 2015). This means that the fields are completely flooded at 10 cm-15 cm depth before planting (usually late April to mid-May), and then seeded with the help of air planes. The fields typically remain flooded throughout the growing season and are only drained from early September onward, approximately 3 weeks before harvest in September to mid-October.

### **2.2.2 Snake River Plain, Idaho**

Idaho accounts for the second largest irrigation water withdrawals in the US after California (NASS, 2012). In Idaho, the Snake River Plain is the most important agricultural area and sprinkler irrigation is the dominant irrigation technique. Similar to the San Joaquin Valley it is characterised by a cold semi-arid climate (Kottek et al., 2006).

### **2.2.3 High Plains, Nebraska**

Nebraska is located in the middle of a transitional climate zone which extends longitudinal through the middle of the US. While the climate in western Nebraska is cold semi-arid, the eastern part is humid-continental, characterised by hot summers and year round precipitation (Kottek et al., 2006). For example, irrigation requirements for corn are around approximately 350 mm in the west and continuously drop to approximately 150 mm in the east (reference values obtained from the University of Nebraska-Lincoln). The mainly employed irrigation system is the centre pivot, and the major crops grown are corn and soybean.

### **2.2.4 Mississippi Flood Plain, Mississippi**

The Mississippi Flood Plain region is characterised by a fully humid subtropical climate with hot summers (Kottek et al., 2006). Despite the large amounts of rainfall throughout the year, only approximately 30% falls in the summer period when the major crops are grown (Kebede et al., 2014), thus requiring the use of supplemental irrigation. The dominant crop types include soybean, corn, cotton and rice. Within the Mississippi Flood Plain we chose an area in the state of Mississippi for a local analysis. Here, reports on irrigation water withdrawals (2009 and 2011 growing seasons) are available from the Yazoo Mississippi Delta Joint Water Management District. For the 2011 growing season, average application rates of approximately 180, 400, 330 and 970 mm are reported for cotton, corn, soybeans and rice respectively, leading to an average of around 490 mm.

## **3 Data sources**

The data sources used in this study are summarised in table 1.

## 3.1 Remotely Sensed Soil Moisture

### 3.1.1 SMAP

The Soil Moisture Active Passive (SMAP) mission was launched in January 2015 and is the second mission exclusively designed for the retrieval of soil moisture together with freeze-/thaw status (Entekhabi et al., 2010). After failure of its radar in July 2015, the radiometer continues to provide measurements in L-band (1.4 GHz) at a spatial resolution of approximately 40 km. Validation studies have shown that the radiometer meets the target retrieval accuracy of  $0.04 \text{ m}^3 \text{ m}^{-3}$  (ubRMSE) over non-frozen land surfaces free of excessive snow, ice, mountainous terrain, and dense vegetation coverage (Colliander et al., 2017). In general, L-band is expected to be ~~most~~ more suitable for soil moisture retrieval, because it is less affected by vegetation and representative of a deeper soil layer than higher frequency C- or X-band retrievals (Entekhabi et al., 2010). SMAP ~~obtain~~ obtains global coverage every 2-3 days and equatorial crossing times are 06:00 and 18:00 local solar time (LST) for the descending and ascending orbits, respectively. We used both ascending and descending orbit data covering the period of April 2015 to December 2016. We used the ~~passive SMAP L3 v4 SM\_P V5 data~~ product, which is sampled at 36 km resolution. In this product version, a water body correction and an improved soil temperature depth correction have been applied, which have respectively reduced anomalous soil moisture values near large water bodies and the dry bias with respect to the SMAP core validation sites (?). In case of overlapping orbits, we only used the descending (06:00 LST) overpass.

### 3.1.2 AMSR2

AMSR2 is a microwave radiometer on board the GCOM-W1 satellite and provides measurements at 6.9 GHz (C-band) and three higher frequencies up to 36.5 GHz (Ka-band) since July 2012 (Imaoka et al., 2010). Daily ascending and descending overpasses are at 13:30 LST and 01:30 LST respectively, achieving global coverage with a spatial resolution of about 40 km every 1-2 days. The VUA-NASA product used in this study is based on the Land Parameter Retrieval Model (LPRM ~~v6~~) V6 algorithm, which simultaneously retrieves volumetric soil moisture and vegetation optical depth (VOD) from the observed brightness temperatures (Owe et al., 2008; der Schalie et al., 2016). LPRM is based on a ~~simple~~ radiative transfer equation and partitions the observation into its emission components from soil and vegetation based on the horizontal and vertical polarised brightness temperatures. ~~The data was~~ Only observations from the descending orbits were used and in addition, the retrievals were masked for high VOD values and radio frequency interference (RFI), spatially resampled to a regular  $0.25^\circ$  grid and temporally centred at ~~12~~ 20:00 UTC (Liu et al., 2012).

### 3.1.3 ASCAT

The Advanced Scatterometer (ASCAT) on board the Meteorological Operational (METOP-A and -B) satellites is operational since October 2006 and is a real aperture radar instrument operating at C-band (5.255 GHz) and VV-polarization. Local equatorial crossing times are at 21:30 for the ascending overpass and at 09:30 for the descending overpass and global coverage is achieved every 1-3 days depending on latitude. The TU Wien change detection algorithm (Wagner et al., 1999; Naeimi

et al., 2009) is applied to the backscatter coefficients to create time series of relative surface soil moisture for the topmost centimetres of soil. This is accomplished by scaling each observation between reference values representing the historically lowest and highest observed backscatter values, respectively. Soil moisture is provided in degree of saturation (%), and ranges between 0% (wilting point) and 100% (soil saturation). It has a spatial resolution of 25 km and is made available on a discrete global grid (DGG) at a spatial sampling of 12.5 km. In this study, we used a modified version of the [EUMETSAT HSAF-European Organisation for the Exploitation of Meteorological Satellites \(EUMETSAT\) Satellite Application Facility on Support to Operational Hydrology and Water \(H SAF\)](#) H111 soil moisture product. The modified version uses a dynamic correction which is expected to better account for inter-annual variability than the original H111 product (Hahn et al., 2017; Vreugdenhil et al., 2016).

### 10 3.2 MERRA-2 reanalysis soil moisture

The second Modern-Era Retrospective analysis for Research and Applications 2 (MERRA-2) (Bosilovich et al., 2015) is an atmospheric reanalysis product providing global, hourly fields of land surface and atmospheric conditions for 1980-present at a spatial resolution of  $0.625^\circ \times 0.5^\circ$ . It assimilates atmospheric satellite observations using the Goddard Earth Observing System Model (GEOS-5). MERRA-2 uses an observation-based precipitation correction over land to fully correct modelled precipitation at [latitudes <math>|<math>42.5^\circ|, with a linear tapering between  \$|42.5^\circ| < \text{latitude} < |62.5^\circ|\$  while no correction is applied at more northern and southern latitudes. The precipitation correction has significantly improved the soil moisture simulations with respect to its predecessor \(Reichle et al., 2017a\). The soil moisture simulations are representative of the first \[10 cm\]\(#\) of soil and are expressed in volumetric units \( \$\text{m}^3 \text{m}^{-3}\$ \). We explicitly chose MERRA-2 soil moisture in favour of soil moisture from other global reanalysis data sets \(e.g. \[ERA-Interim/Land, GLDAS\]\(#\)\), because MERRA-2 does not assimilate surface humidity and surface temperature observations \(Reichle et al., 2017b\), which are directly impacted by irrigation \(Wei et al., 2013; Tuinenburg and Vries, 2017\). \[MERRA-2 surface soil moisture simulations were evaluated in ? with in-situ soil moisture data from 320 sites. It was shown that the modeled estimates are biased by  \\$0.053 \text{ m}^3 \text{ m}^{-3}\\$ , which is approximately in the order of the SMAP soil moisture retrieval target accuracy.\]\(#\)](#)

### 3.3 Ancillary data

25 ~~The~~ [Despite the drawbacks discussed in section 1.2, the](#) ESA CCI Land Cover [data set](#) (Bontemps et al., 2013) was used to create a cropland mask for the CONUS. ~~The cropland classes of the data set represent the period 2008-2012., because the classification of overall agricultural land cover (i.e., irrigated and rainfed lands) proved to be accurate.~~ For a more detailed analysis of the impact of precipitation, we used CPC Unified Gauge-Based Analysis of Daily Precipitation, which covers the CONUS at  $0.25^\circ$  native resolution (Chen et al., 2008; Xie et al., 2010). Therefore, it is expected to provide more detailed information than the precipitation data set used to force MERRA-2 SM, which has a  $0.5^\circ$  resolution.

### 3.4 Data pre-processing

As data from SMAP were only available from April 2015 ~~onwards~~onward, we extended the study period to include available AMSR2 and ASCAT data from 2013 to 2016. Hence, four growing seasons with varying climatic conditions were covered by the AMSR2 and ASCAT sensors, and two growing seasons by SMAP. We assumed a general growing season for the entire  
5 CONUS from the start of April to the end of September. All data were spatially matched to a common  $0.25^\circ$  regular grid using nearest-neighbour resampling. In order to constrain the analysis to areas where irrigation is feasible, we masked all pixels with  $< 5\%$  of fractional cropland area based on ESA CCI land cover for 2010 (Bontemps et al., 2013). Unreliable observations in the satellite data were masked applying their respective quality flags for frozen soil, dense vegetation and radio frequency interference.

10

The spatial representativeness and observation depth slightly differ among the the various remote sensing products and modelled soil moisture. MERRA-2 SM is simulated for a fixed ~~10 cm~~5 cm thick soil layer (Bosilovich et al., 2015) and thus shows more inertia to changes in the water balance (i.e. through precipitation) than the remotely sensing data. Besides, ASCAT is provided in a different unit than the other products. To account for these systematic differences between products, we applied  
15 a linear re-scaling approach (Brocca et al., 2013), which forces the satellite soil moisture time series  $\Theta^{sat}$  to have the same mean  $\mu$  and standard deviation  $\sigma$  as the modelled soil moisture  $\Theta^{mod}$ :

$$\Theta_{rescaled}^{sat} = \frac{\Theta^{sat} - \mu(\Theta^{sat})}{\sigma(\Theta^{sat})} \sigma(\Theta^{mod}) + \mu(\Theta^{mod}) \quad (1)$$

It is likely that over irrigated areas  $\mu(\Theta^{sat})$  increases during the respective irrigation period, which will alter the scaling parameters. We expect that this should not affect the temporal evolution of changes in soil moisture. However, the influence  
20 of irrigation on the temporal variability of soil moisture (depending on the type of irrigation, general climate conditions, etc.) is a source of uncertainty. In particular over very dry regions, the model soil moisture may never reach saturation, while the remotely sensed soil moisture data does (due to irrigation). Since the variable of interest is irrigation amount, volumetric soil moisture in  $\text{m}^3 \text{m}^{-3}$  is converted to the corresponding water column depth  $D_{watertable}$  (mm) by multiplying it with the depth of soil  $D_{soil}$  for which the soil moisture simulations are representative. Thus, for the layer  $0 - \del{10 cm}5 cm, e.g.,  $0.3 \text{ m}^3 \text{ m}^{-3}$   
25 correspond to a ~~30 mm~~15 mm water column covering the unit area of  $1 \text{ m}^2$ .$

## 4 Methods

### 4.1 Theoretical ~~prove of~~foundation for retrieving irrigation water use from microwave remote sensing

Kumar et al. (2015) first proposed the idea of inferring irrigation from a positive bias between remotely sensed and modelled soil moisture, induced by seasonal water application during the dry season. This ideas is based on two key assumptions: first,  
30 the satellite soil moisture products are sensitive to large scale irrigation (as partly confirmed by Escorihuela and Quintana-Seguí (2016); Lawston et al. (2017)) and second, the model does not account for irrigation, neither explicitly (i.e., in the



formulation) nor implicitly through the assimilation of surface humidity or surface temperature observations, which are affected by irrigation (Wei et al., 2013). We build on these assumptions and introduce a new metric to estimate IWU from the difference between satellite-observed and modelled soil moisture. The soil water balance equations describing the respective change in soil moisture for each time step  $t$  [d] are described by

$$5 \quad \frac{d\Theta^{sat}}{dt} = P(t) + I(t) - ET(t) - R(t) - \Delta S_{rest} \quad (2)$$

for the satellite observations and

$$\frac{d\Theta^{mod}}{dt} = P(t) - ET(t) - R(t) - \Delta S_{rest} \quad (3)$$

for the model simulations.  $P$ [mm] is precipitation,  $I$ [mm] is irrigation,  $ET$ [mm] is evapotranspiration,  $\Theta^{sat}$ ,  $\Theta^{mod}$ [mm] are satellite and modelled surface soil moisture, respectively, converted to water column depth.  $\Delta S_{rest}$ [ $m^3 m^{-3}$ ] describes water storage changes below the surface layer, including drainage. Subtracting (3) from (2) yields

$$10 \quad I(t) = \frac{d\Theta^{sat}}{dt} - \frac{d\Theta^{mod}}{dt} \quad (4)$$

Hence, estimating irrigation from differences between the temporal variations of satellite and model SM is theoretically feasible.

## 4.2 Deriving irrigation water use

15 We define an irrigation event as a simultaneous increase in satellite soil moisture ( $\frac{d\Theta^{sat}}{dt} > 0$ ) and a decrease or stagnation in model soil moisture ( $\frac{d\Theta^{mod}}{dt} \leq 0$ ). This means that rainfall did not cause the satellite-observed increase in soil moisture, which over agricultural land was very likely a result of irrigation. For each event, the amount of irrigation water leading to the increase is derived as the difference  $\frac{d\Theta^{sat}}{dt} - \frac{d\Theta^{mod}}{dt}$ , if the change in satellite is significant (i.e. above the noise level). The latter is accounted for by applying a threshold of relative soil moisture change  $thresh_{\Theta}$  (see section 4.3 and appendix A). We then

20 calculate seasonal irrigation water use ( $IWU$ ) summing up the approximated difference quotients over the growing season period:

$$IWU = \int_{i_{SOS}}^{i_{EOS}} (d\Theta_i^{sat} - d\Theta_i^{mod}) dt \approx \sum_{i=SOS}^{EOS} \Delta\Theta_i^{sat-mod} \quad (5)$$

where

$$\Delta\Theta_i^{sat-mod} = \begin{cases} \Delta\Theta_i^{sat} - \Delta\Theta_i^{mod}, & \text{if } \Delta\Theta_i^{sat} \geq \Theta_{thresh} \text{ and} \\ 0, & \text{otherwise} \end{cases}$$

25 with

$$\Delta\Theta_i^{sat} = \Theta_i^{sat} - \Theta_{i-n}^{sat},$$

$$\Delta\Theta_i^{mod} = \Theta_i^{mod} - \Theta_{i-n}^{mod}$$

$IWU$  is the accumulated irrigation water use from the start ( $i_{SOS}$ ) until the end of the growing season ( $i_{EOS}$ ). According to the crop calendars provided by Portmann et al. (2010) and the USDA Planting and harvesting dates handbook (NASS, 2010) the period 1 April- 30 September generally covers the growing season of most crops receiving irrigation water in the CONUS.  $\Theta_i^{sat}$  and  $\Theta_i^{mod}$  are satellite and model SM at day  $i$ ,  $thresh_{\Theta}$  denotes the relative soil ~~mositure~~ moisture threshold and  $\Theta_{i-n}^{sat}$  and  $\Theta_{i-n}^{mod}$  are the last available soil ~~mositure~~ moisture observations with a data gap of  $n$  days. If an irrigation event is detected during an observation gap of  $> 4$  days, we check if there has been a significant increase in the model soil moisture (e.g. due to rainfall) within that period. When more than one significantly positive model slopes (or precipitation events) occur during the gap-period, we cannot say for sure if the observed increase in soil moisture was due to irrigation or precipitation and therefore conservatively disregard the potential irrigation event.

### 10 4.3 Masking spurious irrigation detections

It is essential to differentiate between irrigation signals and high frequency noise in the satellite data. For this purpose, we apply a threshold  $thresh_{\Theta}$  to the relative changes in satellite soil moisture similar to the approach applied by Dorigo et al. (2013) to detect spurious in-situ data:

$$\frac{\Theta_i^{sat} - \Theta_{i-n}^{sat}}{\Theta_{i-n}^{sat}} \geq 0.12 \equiv thresh_{\Theta} \quad (6)$$

15 Based on ~~a~~ an extensive sensitivity analysis (Sect. A) we concluded that a threshold of  $thresh_{\Theta} \equiv 0.12$  is an appropriate generic choice for the whole CONUS.

Potential errors may arise when the model forcing misses or creates false rainfall events. In addition, because of differences in timing of the estimates and differences in represented soil depth between remotely sensed and modelled soil moisture, 20 their response to precipitation events may differ as well. This ~~can~~ may lead to spurious irrigation events when irrigation is estimated at days with rainfall. ~~We therefore used precipitation from MERRA-2 and~~ Therefore, we use information from an additional CPC precipitation data to double-check set at 0.25° resolution, thus providing an approximately 4x higher spatial resolution than the rainfall product used to force MERRA-2 (see section 3.2). This allows us to make a more educated guess when evaluating if the observations and/or model estimates are affected by rainfall ~~and removed them from the analysis if they were.~~ Furthermore, if a potential irrigation signal coincides with preceding rainfall we assume that irrigation is unlikely and disregard the event.

In some extreme cases, capillary rise from deeper soil layers or run-on can wet the top soil. Theoretically, these conditions are reflected by the satellite soil moisture retrievals, but absent in the model soil moisture simulations (i.e. if such effects are not accounted for in the soil hydrology formulation of the LSM (McColl et al., 2017)). However, at the large spatial scales 30 represented by the employed satellite (approximately 25 km) and model soil moisture products (approximately 50 km), very few pixels are expected to show positive  $\Delta\Theta_i^{sat}$  or  $\Delta\Theta_i^{mod}$  in the absence of precipitation or irrigation.

Another impact concerns mismatches between the ancillary data used to force the model and parametrize the respective satellite soil moisture retrieval algorithms, such as land cover and soil parameters. By rescaling to the model dynamic soil

moisture range, we implicitly account for mismatches in soil parameters. However, addressing potential mismatches in land cover was out of the scope of this paper and thus represent an intrinsic limitation of the method.

## 5 Results and Discussion

### 5.1 Growing season correlations between satellite and model soil moisture

- 5 To investigate the potential detectability of IWU, we investigated the correlation between satellite and modelled soil moisture during the growing season ((Figure 3). We computed the correlation separately for dry (precipitation= 0;  $\bar{r}_{dry}$ ) and wet conditions (precipitation > 0;  $\bar{r}_{wet}$ ). If  $\bar{r}_{dry}$  is low or negative over agricultural areas which are known to be irrigated (as inferred from the MIRA-AD-US product) while  $\bar{r}_{wet}$  is strongly positive, this is a strong indication of irrigation.
- 10 Over non-agricultural land cover, low growing season correlations between SMAP and MERRA-2 soil moisture are observed over the densely vegetated south- and north-eastern US, and over parts of the arid south-west (Figs. 3a, 3b). AMSR2 exhibits low correlations in coastal areas, complex terrain and over dense vegetation cover (Fig. 3c, 3d). ASCAT shows negative correlations against MERRA-2 over the arid south-western deserts and the densely vegetated coastal north-west and south-east (Fig. 3e, 3f). Overall, for each satellite-model pair there is a clear reduction of  $\bar{r}_{dry}$  with respect to  $\bar{r}_{wet}$  over several irrigation
- 15 hot spots within the CONUS.

#### 5.1.1 Central Valley

- Over the Central Valley, SMAP shows moderate to high  $\bar{r}_{wet}$  with MERRA-2, except for the Sacramento Valley in northern California. In contrast,  $\bar{r}_{dry}$  is moderately to strongly negative over the southern San Joaquin Valley, which indicates that an irrigation signal is indeed observed by the satellite sensor. The fact that  $\bar{r}_{dry}$  is comparable, if not higher than  $\bar{r}_{wet}$  over
- 20 the Sacramento Valley should be attributed to the special characteristics of the prevalent rice irrigation. In the Sacramento Valley, a permanent flood of 10-15cm is usually maintained during the whole growing season before fields are drained in preparation for harvest (Linguist et al., 2015). Hence, irrigation water remains observable during both wet- and dry periods of the growing season, and the impact of irrigation on  $\bar{r}$  actually increases for the wet period with respect to the dry period. In contrast, ASCAT exhibits high correlations with MERRA-2 in this region. ~~This may be due~~ During the early phenological
- 25 growth phase of rice, this observation can be attributed to specular reflection of the radar signal from the ~~rice, which would~~ cause a signal that looks similar to one coming from a dry soil-flood water surface, given that wind speeds do not significantly affect the water's surface roughness (Nguyen et al., 2015). By the time the rice stems start to break through the water surface the now elongated rice stems are known to act as double-bounce reflectors, which commonly results in an enhanced backscatter signal that can be observed until field drainage in late summer (??) (see ASCAT soil moisture time series in figure 5b). Both
- 30 SMAP and ASCAT show moderate to high negative correlations against MERRA-2 in the heavily irrigated San Joaquin Valley. Concerning AMSR2 SM there is no clear pattern of discrepancy between  $\bar{r}_{wet}$  and  $\bar{r}_{dry}$  in the Central Valley.

### 5.1.2 Snake River Plain

Over the Snake River Plain, ASCAT has a clear signal that could be attributed to irrigation. Particularly in the central and western-most areas along the Snake River,  $\bar{r}_{dry}$  depicts a strong negative correlation with MERRA-2, while  $\bar{r}_{wet}$  is moderately positive. Moderately negative  $\bar{r}_{dry}$  obtained for SMAP shows a good alignment with areas known to be irrigated in the Snake River Plain. Although the correlation is less negative than for ASCAT, the spatial pattern is resembled more clearly. Here, AMSR2 shows slightly more negative  $\bar{r}_{dry}$  than  $\bar{r}_{wet}$  over agricultural land cover, but the spatial pattern appears to be less reliable than for the other satellite products.

### 5.1.3 High Plains

The ASCAT product is the only one to show a distinct pattern of negative correlation over the irrigated part of the Nebraska Plains. While  $\bar{r}_{wet}$  shows weak positive correlations,  $\bar{r}_{dry}$  reveals strong negative  $\bar{r}$ , suggesting that an irrigation signal is entailed in the ASCAT signal. However, this pattern cannot be reliably attributed to irrigation practices as ASCAT shows low correlations over the entire Corn Belt region, where agriculture is generally known to be rain-fed (see Fig. 2). Vegetation scattering effects from the corn canopies are a plausible explanation for the observed deviation. As the corn plants reach their maximum height (up to approximately 3m) towards the end of the growing season, the C-band backscatter signal will increasingly be composed of canopy backscatter and canopy-soil double bounce reflections, while sensitivity to actual soil moisture decreases (Daughtry et al., 1991; Joseph et al., 2010).

### 5.1.4 Mississippi Flood Plain

Lastly, all products show low  $\bar{r}$  values over the Mississippi Flood Plain, although with varying magnitudes. In this region, ASCAT shows the lowest negative correlation, followed by AMSR2 and SMAP. Moreover, for all SM products  $\bar{r}_{dry}$  is lower than  $\bar{r}_{wet}$ .

### 5.1.5 Other regions

Figure 3 also reveals that strong negative  $\bar{r}_{dry}$  (in combination with moderately high  $\bar{r}_{wet}$ ) based on ASCAT align well with areas known to be irrigated over the Columbia River Basin, Washington. [As the ASCAT soil moisture product has a significantly higher nominal spatial resolution than the passive products, we hypothesise that in this region it is the only sensor to resolve the irrigation practices.](#) Correlations based on SMAP loosely agree with this pattern and AMSR2 only has few valid observations over this region. In addition, both ASCAT and SMAP have patterns of  $\bar{r}_{dry} < \bar{r}_{wet}$  over an irrigated region in south-western Georgia. In contrast, AMSR2 shows moderately high positive  $\bar{r}$  over this region.

To determine the sensitivity of the growing season correlation  $\bar{r}$  between satellite and model soil moisture to variations in fractional irrigated area within a pixel, we examined their relationship with irrigation intensities derived from the MIRAD-US irrigated area data set (Pervez and Brown, 2010). However, no evidence of a negative linear relationship between the two

variables was found (not shown), as at low irrigation fractions  $\bar{r}$  is mostly dominated by effects originating from the remaining land cover types. Overall, the results obtained by separately analysing the spatial patterns of  $\bar{r}_{dry}$  and  $\bar{r}_{wet}$  between satellite and model soil moisture largely support the hypothesis that over areas known to be irrigated, the remotely sensed soil moisture signal deviates from modelled soil moisture, given that the model does not explicitly account for irrigation (which is the case for MERRA-2). Hence, the overall hypothesis of this study, which is that IWU can be inferred from differences between the temporal variations of the remotely sensed and modelled soil moisture is corroborated.

## 5.2 Spatial patterns of estimated irrigation water use

Spatial plots of mean annual estimated irrigation water use  $\overline{IWU}$  (i.e. averaged over the study period of 2013-2016) (Figs. 4a-4c) suggest that all satellite products are able to identify the extensive irrigation applied in the California Central Valley. Here, SMAP derived  $\overline{IWU}$  clearly resembles the irrigation patterns of the MIRA-AD-US data set in the northern Sacramento Valley and southern San Joaquin Valley (Fig. 2). AMSR2 and ASCAT derived  $\overline{IWU}$  is generally higher than SMAP and extends throughout the whole California Central Valley. Although small in magnitude, the  $\overline{IWU}$  pattern derived from ASCAT over the central Snake River Plain is spatially distinct. Similarly, AMSR2 shows a clear signal over the western to central Snake River Plains. Concerning the Nebraska Plains, only AMSR2  $\overline{IWU}$  shows patterns that agree with the MIRA-AD-US. Over the Mississippi Flood Plain, ASCAT shows the highest  $\overline{IWU}$ , followed by AMSR2.

ASCAT-derived  $\overline{IWU}$  seems to be affected by vegetation effects in the Corn Belt region and in the south-eastern US. For all sensors, the method fails to detect  $\overline{IWU}$  in many irrigated areas, especially those along the High-Plains-Aquifer (Nebraska, Kansas, Texas), which extends from the northern to the southern central US. A plausible explanation for missing these areas is that many farmers in these regions practice supplemental irrigation, thus resulting in a less distinguishable irrigation signal. In addition, the centre pivot irrigation systems, which are mainly used in this region, have much higher water application efficiencies compared to the flood- and furrow irrigation systems used in the Sacramento Valley and Mississippi Flood Plain (see Fig. A1). Rainfall seasonality is another potential reason for the underestimation in the central U.S, where the climate transitions from arid in the west to humid in the east. To investigate it's impact, we plotted the average number of days per growing season where  $IWU > 0$  (figure A3), which sums up to the number of days that went into the  $\overline{IWU}$  estimates shown in figure 4. It can be seen that for SMAP based  $IWU$ , a significant number of days with irrigation (mean count) only is detected in the arid west and south-west. For AMSR2, the mean counts are highest in California, although counts in the range of 20-30 occur in the Snake River Valley, Mississippi Flood Plain and other agricultural regions. In agreement with the passive products, mean counts for ASCAT are highest in California and south-western states. There also is a clear pattern in the Mississippi Valley and along the south-eastern states.

Furthermore, the global relative chosen global threshold of  $thresh_{\Theta} = 12\%$  also masks irrigation signals in regions such as the Columbia River Basin, Washington (results not shown) where the noise level of the satellite soil moisture retrievals is

rather low (see section A2). Thus, a more site-specific threshold at each pixel might lead to ~~improved-detectability~~ an improved detectability of irrigation events.

### 5.3 Temporal behaviour of soil moisture and IWU and in the four focus regions

For a more detailed analysis on the impact of climate, crop type, and irrigation practice on the method performance, we compared remotely sensed and modelled soil moisture time series, and monthly *IWU* estimates at an irrigated (green crosses in Fig. 2) and a non-irrigated pixel (orange crosses in Fig. 2) in the four focus areas (Fig. 5).

#### 5.3.1 Central Valley

At the irrigated pixel in the San Joaquin Valley, the impact of irrigation on the remotely sensed soil moisture signal is evident (top panel in Fig. 5a). While MERRA-2 soil moisture decline in the irrigated and non-irrigated pixels reflects the absence of precipitation, typically from mid-May until mid-October, ASCAT and SMAP soil moisture in the irrigated pixel start to increase in June until reaching their maximum in July-August and gradually declining towards the end of the growing season. In contrast, remotely sensed soil moisture in the adjacent non-irrigated pixel (bottom panel) remains close to zero throughout the growing season. The temporal behaviour of SMAP at the irrigated pixel location was extensively evaluated by Lawston et al. (2017), who showed that SMAP soil moisture correctly reflects the onset of flood irrigation, the dry down associated with plants breaking through the water surface (which attenuates the SM signal), and lastly field drainage. Even though Lawston et al. (2017) used the enhanced 9 km sampling SMAP product, we find very comparable temporal characteristics for the native 36 km resolution product (Fig. 5b). ASCAT soil moisture seems to be impacted by specular reflection of the active radar signal from the flooded rice fields, leading to very low backscatter and, hence, soil moisture values. As a result, particularly during the 2013 growing season ASCAT soil moisture remains at- or very close to its minimum early in the growing season. ASCAT soil moisture starts to increase in early to mid-July when the rice starts to break out of the water. Initially, the increase is primarily the result of double-bounce effects from the rice canopies, while at later growth stages this turns into volume scattering (Nguyen et al., 2015). Of the three products, ASCAT soil moisture is the last to reach its growing season maximum between mid- to late August, followed by a decrease throughout September. At the irrigated pixel, AMSR2 soil moisture shows large fluctuations during the growing season, while at the non-irrigated pixel it has few valid observations, which makes it difficult to compare both pixels. AMSR2 soil moisture shows similar characteristics with respect to SMAP and is able to sense the onset of flood irrigation, but reaches saturation a few weeks earlier and already starts to dry down before SMAP reaches its soil moisture maximum. Moreover, after reaching a minimum in late July to early August, AMSR2 soil moisture starts to increase again.

Comparing the estimated monthly *IWU* (bottom sub-panels) at the adjacent irrigated and non-irrigated pixels suggests that the method is skillful in detecting irrigation from all considered sensors, especially during the comparatively dry years of 2013 and 2014, when a prolonged drought affected the state of California. AMSR2 provides highest *IWU* estimates, possibly due to the high noise levels in the soil moisture data. In general, a spurious irrigation signal remains at the non-irrigated pixel, which may be due to noise in the satellite soil moisture retrievals. At the non-irrigated pixel, ASCAT- and AMSR2-based

IWU retrievals seem to be more affected by noise than SMAP. The 2015 growing season was unusually wet, which at the non-irrigated pixel in the spurious detection of irrigation for all satellite products. Generally, especially SMAP and ASCAT products are skillful in detecting the seasonality of irrigation over the San Joaquin Valley.

### 5.3.2 Snake River Plain

5 At Snake River Plain, all satellite soil moisture products show a clear irrigation signal at the irrigated pixel (Fig. 5c), which is not visible in the non-irrigated pixel. Consequently, considerable IWU is estimated for the irrigated pixel, while for ASCAT and SMAP the estimated IWU at the non-irrigated pixel is close to zero. AMSR2 soil moisture retrievals are noisier, which results in the detection of some spurious irrigation at the non-irrigated pixel, although significantly smaller than at the irrigated pixel. We argue that the higher spatial sampling of the employed ASCAT data is advantageous for IWU estimation, as the  
10 irrigated area within the Snake River Plain is quite narrow.

### 5.3.3 High Plains

ASCAT soil moisture content is higher than MERRA-2 during the drier periods of the growing season, indicating sensitivity to the typically employed supplemental irrigation (Fig. 5d). However, the relative changes in ASCAT soil moisture are  $< 12\%$  and therefore do not qualify as rigorous irrigation events based on our methodology. AMSR2 provides the largest derived IWU  
15 at the irrigated pixel, but is also affected by noise at the non-irrigated pixel. In this area, the influence of irrigation on the remotely sensed soil moisture signal is much more subtle, if significant at all. This can be attributed to two factors: First, due to the abundant rainfall during the growing season only supplemental irrigation is applied in this area. Second, center-centre pivot irrigation systems usually have much higher application efficiencies (75 – 95%) than gravity irrigation systems (40 – 80%). Therefore, less water needs to be applied to achieve comparable plant growth, rendering a less distinct irrigation signal in the  
20 soil moisture product.

### 5.3.4 Mississippi Flood Plain

The difference in soil moisture behaviour between the irrigated and non-irrigated pixel is much more pronounced for AMSR2 than for the other satellite products (Fig. 5e). This is also reflected by AMSR2-derived IWU at the irrigated pixel, which agrees well with the expected seasonality of irrigation, which peaks in August. At the same time AMSR2-based IWU estimates are  
25 close to zero at the non-irrigated pixel. ASCAT soil moisture shows a similar seasonality at the irrigated pixel, but is more affected by noise at the non-irrigated pixel. SMAP soil moisture sustains saturation throughout the first half of the growing season, which could be either caused by flood irrigation for rice, or point at a problem in the soil moisture retrieval algorithm. At least for AMSR2, IWU shows a meaningful derived seasonality.

## 5.4 Evaluation of estimated irrigation water use against state-level reference water withdrawals

We evaluated the agreement between mean IWU  $\overline{IWU}$ , aggregated for each satellite-model pair to the state level, and reported irrigation water withdrawals from the 2013 FRIS (USDA, 2013) ( $IWW_{FRIS}$ ). The median correlation  $R$  values for SMAP-, AMSR2- and ASCAT-based  $\overline{IWU}$  and  $IWW_{FRIS}$  are ~~0.79~~0.80, 0.56, and 0.36, respectively. For all satellite ~~datasets~~data  
5 sets, California is correctly identified as the largest consumer of irrigation water, which indicates the overall potential of coarse resolution microwave soil moisture data in estimating  $IWU$ . However, the root-mean-squared-difference (RMSD) and bias between observed  $\overline{IWU}$  and  $IWW_{FRIS}$  indicate a clear underestimation. The lowest RMSD of ~~5.01 km<sup>3</sup>~~5.21 km<sup>3</sup> was found for AMSR2, but values for SMAP and ASCAT are ~~very quite~~ similar. ASCAT has the lowest bias (~~-2.06 km<sup>3</sup>~~-2.29 km<sup>3</sup>), but the bias based on the other products are similar. We further discuss the potential reasons for the generally large biases observed  
10 in section 5.6. On average,  $\overline{IWU}$  based on SMAP provides the closest similarity with  $IWW_{FRIS}$ .

## 5.5 Evaluating irrigated area estimates with the MirAD-US data set

We compared spatial patterns of total ~~average mean~~  $\overline{IWU}$  estimates with the MirAD-US data set at 0.25 ~~resolution. To be able~~  
° resolution. In order to compute a confusion matrix, we converted the continuous ranges of the two data sets into binary representations of irrigated areas. For MirAD-US, this was accomplished by labelling only areas with  $\geq 5\%$  irrigation fraction  
15 as irrigated. Estimated  $\overline{IWU}$  was converted in a similar way by considering only pixels where  ~~$\overline{IWU} \geq 20\text{mm}$  as irrigated.~~  
~~To comparing~~  $\overline{IWU} \geq X$  as irrigated, where  $X(\text{mm})$  is a binarisation threshold. To compare irrigation estimated from each satellite-model pair with MirAD-US, we computed the error of omission (EoO), the error of commission (EoC), the overall accuracy (OA), and Cohen's kappa ( $\kappa$ ), which is a measure of how the classification results compare to values assigned by chance (Table 2). The binarisation threshold  $X$  was determined by maximizing  $\kappa$  for each satellite-model pair and focus region  
20 respectively, as well as for the whole CONUS (see figure A5).

In California, irrigated area estimates based on  $\overline{IWU}$  ~~shows~~ show very good agreement with MirAD-US. SMAP-based irrigated areas provides the highest scores for all metrics: the overall accuracy (OA) is ~~77.68~~76.79%. A commission error (EoC) of ~~21.43~~23.30% in combination with an omission error (EoO) of ~~4.94~~2.47% indicates that we somewhat overestimate the reference and a kappa score of  $\kappa = 0.33$  illustrates a fair agreement. ASCAT has a similar performance, but shows a slightly higher overestimation ( ~~$EoC = 24.51\%$~~  $EoC = 22.68\%$ ), thus resulting in a lower overall accuracy and  $\kappa$  score. In California, AMSR2 performs worst, but still shows an acceptable overall accuracy of 68.75%. In Idaho, of all satellite products AMSR2 ~~clearly~~  
25 shows the highest agreement with the reference ( ~~$OA = 59.02\%$~~  $OA = 59.84\%$ ), but  $EoC$  and  $EoO$  are equally high at approximately ~~41~~40%, indicating a moderate amount of confusion in the classification. As a result of a strong under-classification, in  
30 Nebraska there is hardly any agreement between IWU-based and MirAD-US irrigated area. Over the Mississippi Flood Plain, ~~AMSR2-based IWU shows good (among the products by far the best)~~ AMSR2 and ASCAT-based IWU shows moderately good agreement with the reference data ( ~~$OA = 71.11\%$ ,  $\kappa = 0.32$~~  $OA \approx 70\%$ ,  $\kappa > 0.30$ ). We argue that, due to the previously observed problems regarding the representation of soil saturation, ~~both ASCAT and~~ SMAP soil moisture data are unreliable



in this region. ASCAT-based IWU depicts a high over-estimation ( ~~$EoC = 62.65%$~~  $EoC = 50%$ ) while SMAP-based IWU does not classify any irrigated areas at all ( $EoO = 100%$ ). For CONUS as a whole, ~~SMAP depicts the best~~ ASCAT and SMAP depict the best spatial agreement with MIrAD-US irrigated area, which is reflected by an overall accuracy of ~~74.03%~~ 74.55% and 72.96% respectively. However, SMAP fails to correctly classify approximately 90% of areas irrigated according to the MIrAD-US. AMSR2 shows ~~the second best agreement ( $OA = 66.82%$ )~~ an agreement of  $OA = 59.38%$  and misses fewer pixels than ~~SMAP ( $EoO = 72.7%$ )~~ ASCAT and SMAP ( $EoO = 49.63%$ ), but in contrast shows a higher over-estimation ( ~~$EoC = 67.64%$~~ ). ASCAT shows the lowest agreement with an  $OA$  of  $61.88%$ .  $EoC = 68.37%$ .

The results obtained for California are encouraging and emphasise the potential of coarse scale microwave soil moisture retrievals in correctly detecting the spatial patterns of irrigation. However, consistent with the findings of estimated irrigation volumes, irrigated area estimates reflect a general pattern of underestimation with respect to the MIrAD-US data set. The results further indicate that in areas such as Nebraska, where the climate is semi-humid in large parts of the state and irrigation is mostly supplementary, the method fails in detecting the irrigation signal.

## 5.6 Sensitivity of microwave soil moisture products to irrigation

By qualitatively examining the obtained results, we find that the sensitivity of the employed microwave soil moisture retrievals to irrigation and the performance with respect to reported irrigation data particularly depend on the following factors:

### 1. Spatial resolution of the microwave soil moisture products and topography

Likely, the largest restriction is the coarse scale of the satellite soil moisture retrievals with respect to the average field size. For instance, the area irrigated by a typical centre pivot system (i.e. 500 m) is approximately 50 ha, which only accounts for approximately 0.0003 % of the satellite footprint area. Thus, around 3200 centre pivot systems are needed to create a uniformly irrigated area covering the remotely sensed footprint. In the CONUS, areas with large irrigation fractions exist in the eastern half of the country, but irrigation in the arid western half is a lot more heterogeneous. In these areas, irrigation usually mainly depends on surface water supply and is therefore reserved to narrow river valleys such as the Colorado River valley. As a consequence, coarse scale microwave soil moisture products may be insensitive to locally significant (but insignificant with respect to the scale of the satellite footprint) irrigation due to the small scale of the irrigation practices and surrounding complex topography (e.g. mountains, valley-transitions, water bodies). ~~However,~~ As discussed in section 5.1, in the Columbia River Basin correlation patterns based on the ASCAT soil moisture product (which has a significantly higher nominal spatial resolution than the passive products) matched very well with the MIrAD-US product. An investigation of time series over this region (not shown) revealed that there, ASCAT soil moisture carries a distinct seasonal irrigation signal. The reason why this pattern cannot be observed in figure 4c is that the regional noise level is well below the global threshold and thus irrigation is actually being masked. Lastly, as depicted by figure A1 ~~and the latest Agricultural Census from USDA~~, irrigation water application rates are the highest

in arid climates. We therefore expect that these drawbacks significantly contribute to the underestimation of reported irrigation water withdrawals.

## 2. Climate

As discussed in section A, the method in its current formulation is only applied to rain-free periods during the growing season. We believe that this constraint accounts for a substantial part of the underestimation of  $\overline{IWW}$  with respect to reported  $IWW$ . If rainfall cannot meet the plant's total daily evaporative demand, farmers may decide to irrigate even at rainy days. Actual, farmers often irrigate at days with rainfall, at which evapotranspiration rates are lower and, hence, irrigation water loss decreases. Nevertheless, we did not come up with an adequate way of decomposing the impact of rainfall and irrigation in the soil moisture signal on a daily basis. At daily temporal sampling, in some cases satellite and model soil moisture show markedly different responses to precipitation events both in terms of temporal characteristics and intensity. This results in spurious irrigation events, which motivated us to constrain the method to dry periods. When full irrigation is applied in arid climates, the microwave soil moisture retrievals generally show promising skills in detecting the irrigation signals. In contrast, for the predominantly semi-humid climate (e.g. High Plains and Mississippi Flood Plain) irrigation mainly aims at increasing yield or bridging dry periods (i.e. supplementary irrigation). Consequently, less irrigation water is applied and thus the microwave soil moisture retrievals may not appropriately capture less pronounced soil wetting.

## 3. Crop type and irrigation system

Water requirements naturally vary between crop types. Of the main crop types grown in the CONUS, alfalfa and rice typically require most irrigation water. Particularly flood irrigation for rice leads to a strong irrigation signal in the Sacramento Valley. The signal of flood irrigation is less distinct in the semi-humid climate of the Mississippi Flood Plain, yet SMAP sensed a prolonged period of soil saturation which may be attributed to flooded fields (section 5.3, Fig. 5e). However, the consistent rainfall in this region reduces the method performance, as the irrigation and precipitation signals in the soil moisture data cannot be disentangled. On the other hand, the extensive supplementary irrigation applied by centre pivot systems in the High Plains does result in a minor irrigation signal in the soil moisture retrievals (section 5.3, Fig. 5d). Intriguingly, the same dynamic was observed for other irrigated areas along the Ogallala Aquifer (Kansas, Oklahoma, Texas; not shown).

We suggest that the differences in detectability may be related to the application efficiency of a particular irrigation system, which is defined as the ratio between the average low quarter depth of water added to root zone storage and the average depth of water applied to the field (in mm) (Pereira et al., 2002). Gravity irrigation systems have the lowest efficiency (approximately 60 %), followed by sprinkler- (approximately 75 %), and micro-irrigation systems (approximately 90 %). Consequently, microwave soil moisture retrievals are expected to be most sensitive to flood irrigation, followed by sprinkler- and micro-irrigation. The highest irrigation water consumption per area occurs in the arid-west and-western parts of the CONUS, particularly in the south-west (Fig. A1. Besides, ~~each farmer separately controls his~~

~~fields and focuses~~ farmers separately control their fields and focus on a different variety of crops based on market conditions, which in turn require different irrigation amounts and timing. This means that between satellite overpasses only a fraction of the fields within the satellite footprint will have received irrigation (based on the individual water management of each farmer). In addition, a centre pivot irrigation system takes between 12-24 hours to complete a full rotation circle, which means that at the time of satellite overpass only a fraction of a field has recently received irrigation. The same is true for other irrigation techniques, as irrigation equipment (e.g. pipes) has to be manually transferred across fields.

#### 4. Satellite observation system and wavelength

Our results indicate that the observation system (i.e. active or passive remote sensing system) have an impact on the sensitivity of soil moisture retrievals to irrigation. For instance, the water applied by certain types of irrigation (i.e. flood irrigation for rice) could not be comprehensively detected by the active ASCAT sensor due to specular reflection of the radar signal (see section 5.3, Fig. 5b). On the other hand, the active microwave data provided valuable information on the timing of both flood irrigation onset and field drainage and additionally allowed insights into the crop development cycle (i.e. backscatter increases when the vegetation starts to break through the standing water surface, potentially causing double bounce effects (Nguyen et al., 2015)). These dynamics largely agree with the observations reported by Lawston et al. (2017). Regarding the observation wavelength, we found that the SMAP L-Band data showed more sensitivity than AMSR2 C-band to the flood maintenance flow that is commonly established after the start of the growing season at the rice-irrigated site in the Sacramento Valley, California. However, we cannot safely conclude if this is actually due to the observation wavelength or to differences in the retrieval algorithms.

## 6 Conclusions and Outlook

In this paper we presented a new methodology to derive irrigation water use at monthly time scales by combining microwave remote sensing and modelled soil moisture data. We first assessed if irrigation impacts the correlation between remotely sensed and modelled soil moisture and found that the growing season correlations between each satellite-model pair (SMAP, AMSR2, and ASCAT against MERRA-2) are significantly lower over major irrigation areas throughout the CONUS. Hence, deriving IWU from differences between satellite and model data is theoretically possible. We then derived IWU estimates over the CONUS for the period 2013-2016 and evaluated our estimates, aggregated per state, with reports on state-level irrigation water withdrawals from the 2013 Farm and Ranch Irrigation Survey (USDA, 2013). Of all satellite products, SMAP-derived IWU showed the highest correlation between state-aggregated observed and reported irrigation volumes ( $r=0.79$ 0.80), followed by AMSR2 ( $r=0.56$ ) and ASCAT (0.36). Moreover, we compared the spatial IWU patterns against the MIrAD-US dataset (Pervez and Brown, 2010). Again, SMAP-derived IWU patterns showed highest agreement with the MIrAD-US, followed by AMSR2 and ASCAT.

However, for all satellite products, derived IWU is significantly lower than reported irrigation water withdrawals. In line with previous studies (Escorihuela and Quintana-Seguí, 2016), we argue that this discrepancy can be mainly attributed to the coarse

resolution of the satellite soil moisture retrievals, which in many regions does not allow for resolving the irrigation signal at the field scale, or for areas of small scale irrigation. Besides, the derived IWU relies on the quality of the soil moisture observations, which are impacted by topography, vegetation effects, instrument noise, and the observation principle itself (active versus passive microwave observations). Furthermore, the ability to extract IWU is controlled by the sensitivity of the overall soil moisture signal to irrigation, which is driven by the type and frequency of irrigation, its timing with respect to the satellite overpass, and climate. For example, our method failed to detect IWU in areas with humid growing seasons where irrigation is only supplemental. Despite these major drawbacks, we found that the seasonality of observed irrigation water use is meaningful over several irrigation hot spots such as the California Central Valley, the Snake River Plain, and the Mississippi Flood Plain.

Many of the current limitations can be overcome by using imagery of higher spatial resolution (providing improved capacity to resolve the local irrigation signal within the satellite footprint area) and temporal resolution (providing observations closer to the actual irrigation time). Suitable candidates are e.g., the spatially interpolated SMAP enhanced 9 km product (Chan et al., 2018), the SCATSAR-SWI product with a 1 km spatial and daily temporal resolution obtained from the fusion of active microwave remote sensing 25 km Metop ASCAT soil moisture (Bauer-Marschallinger et al., 2018), or soil moisture products at approximately 1 km based on Cyclone Global Navigation Satellite System (CYGNSS) (Chew and Small, 2018). Also multi-satellite products, such as the ESA Climate Change Initiative Soil Moisture product (Dorigo et al., 2017; Liu et al., 2012) offer a great potential to increase spatial and temporal resolutions, provided that the original soil moisture variations are maintained in the merged product.

Despite the current limitations observed, our findings highlight the potential of using microwave soil moisture retrievals for estimating intra- and inter-annual variations in actual IWU and indicate the overall usefulness of the proposed method. IWU estimates based on microwave soil moisture observations can provide both stand-alone information and synergistic value in combination with methods commonly used to estimate irrigated area or potential evaporative demand from optical or thermal data. Based on past and current microwave satellite missions, remotely sensed soil moisture has the potential to provide information on irrigation water use over the last four decades, which can be used to force climate models and assess the impact of irrigation on regional climate.

## Appendix A: Optimization of the noise threshold $thresh_{\Theta}$

### A1 Optimization based on the correlation of estimated irrigation water use with reported water withdrawals

We examined how different  $thresh_{\Theta}$  values affect the agreement between observed IWU and reported irrigation water withdrawals  $IWW_{FRIS}$ . For this purpose, annual mean irrigation water use  $\overline{IWU}$  derived from each satellite-model pair by applying different thresholds was aggregated at the state-level and compared to reported irrigation water withdrawals  $IWW_{FRIS}$  from the 2013 FRIS (USDA, 2013) (Table A1). It is important to point out that there is a temporal mismatch, however these data were the most up to date official reference covering the whole CONUS. The correlation coefficient  $R$

between observed  $\overline{IWU}$  and  $IWW_{FRIS}$  for SMAP is 0.72 when using  $thresh_{\Theta} = 0.04$ , but much smaller for AMSR2 (0.35) and ASCAT (0.15). When increasing  $thresh_{\Theta}$  to 0.08,  $R$  increases for all soil moisture products (0.79 0.47, 0.23 for SMAP, AMSR2, and ASCAT, respectively).  $thresh_{\Theta} = 0.12$  further increases correlations to 0.80, 0.56, and 0.36 for SMAP, AMSR2, and ASCAT SM respectively. However, with an increase of the correlation coefficient, the bias and RMSD progressively increase. For this reason, the final threshold  $thresh_{\Theta} = 0.12$  is a trade-off of optimal correlation, bias, and RMSD.

## A2 Optimization based on soil moisture time series in the four focus-regions

~~We apply~~ To further investigate the plausibility of the choice of  $thresh_{\Theta}$  in Sect. 5.4 at pixel scale and in several climatic settings (i.e., in the chosen focus regions), we applied a minimum threshold  $thresh_{\Theta}$  to separate increases in soil moisture stemming from ~~true-actual~~ irrigation from disturbing impacts like ~~dataset-data set~~ noise. We optimised  $thresh_{\Theta}$  by maximising the relative difference between IWU estimated at an irrigated ( $PI$ ) and a non-irrigated pixel ( $PNI$ ) in each focus area (Sect. 2.2) and for each satellite product. ~~This is done through the following function~~ By assuming that those locations are spatially correlated in terms of climate and land cover, doing so allows us to find the minimum  $thresh_{\Theta}$  where the estimated irrigation at the non-irrigated location actually is zero. This is accomplished by minimising the cost function  $h(IWU)$ :

$$h(IWU) = \frac{\overline{IWU}_{PNI} - \overline{IWU}_{PI}}{\overline{IWU}_{PI}} \rightarrow \min. \quad (A1)$$

where  $\overline{IWU}_{PI}$  and  $\overline{IWU}_{PNI}$  are mean annual IWU estimated at  $PI$  and  $PNI$  respectively (Fig. A4). ~~Even~~ It can be seen that the minimum thresholds vary across regions, indicating the range of noise levels within the respective soil moisture retrievals. In the scope of this study however, we chose a global threshold and even though there is no single  $thresh_{\Theta}$  that leads to a minimum for all sensors and all focus areas, similarly to section 5.4, we find an overall mean  $thresh_{\Theta}$  of 0.11 - 0.12 across the focus regions, which supports the choice made in section A1. Moreover, the data clearly show that SMAP soil moisture has a lower noise level (no data points mean that  $\overline{IWU}_{PNI}$  is zero) in comparison with AMSR2 and ASCAT soil moisture across the different climatic conditions and irrigation practices reflected by the four focus regions. The reason why the estimated IWU at the  $PNI$ s is non-zero is two-fold: First, the true spatial resolution of the satellite SM products (approximately 40 km for SMAP and AMSR2, approximately 25 km for ASCAT) is coarser than the spatial sampling of the common data grid (25 km) and thus, if the choice of  $PNI$  is very close to  $PI$ , the soil moisture retrieval at  $PNI$  may as well be affected by irrigation. Second, noise or deficiencies in the soil moisture retrieval can result in spurious irrigation signals.

## A3 Optimization based on the correlation of estimated irrigation water use with reported water withdrawals

To supplement the local optimization analysis, we examined how different noise  $thresh_{\Theta}$  values affect the agreement between observed  $\overline{IWU}$  and reported irrigation water withdrawals  $IWW_{FRIS}$ . For this purpose, annual mean irrigation water use  $\overline{IWU}$  derived from each satellite-model pair by applying different thresholds was aggregated at the state-level and compared to reported irrigation water withdrawals from the 2013 FRIS (USDA, 2013) (Table A1). The correlation coefficient  $R$  between observed  $\overline{IWU}$  and  $IWW_{FRIS}$  for SMAP is 0.65 when using  $thresh_{\Theta} = 0.04$ , but much weaker for AMSR2 (0.35) and ASCAT (0.15). When increasing  $thresh_{\Theta}$  to 0.08,  $R$  increases for all soil moisture products (0.75 0.47, 0.23 for SMAP,

AMSR2, and ASCAT, respectively).  $thresh_{\Theta} = 0.12$  further increases median correlations to 0.79, 0.56, and 0.36 for SMAP, AMSR2, and ASCAT SM respectively. However, with an increase of the correlation coefficient, the bias and RMSD progressively increase. For this reason, the final threshold  $thresh_{\Theta} = 0.12$  is a trade-off of optimal correlation, bias, and RMSD.

*Competing interests.* None

- 5 *Acknowledgements.* Felix Zaussinger, Wouter Dorigo and Alexander Gruber received funding from the European Union Seventh Framework Programme (FP7/2007-2013) under grant agreement number 603608, „Global Earth Observation for integrated water resource assessment“: earth2Observe. In addition, Wouter Dorigo acknowledges the TU Wien Wissenschaftspreis. Luca Brocca, Angelica Tarpanelli and Paolo Fillipuchi received funding from the „WACMOS-Irrigation“ project under grant agreement number ESA EXPRO RFP/3-14680/16/I-NB. In addition, the authors acknowledge the TU Wien University Library for financial support through its Open Access Funding Program.
- 10 *Data availability.* Data from the ESA CCI Landcover project is available under <https://www.esa-landcover-cci.org/>. CPC US Unified Precipitation data was provided by the NOAA/OAR/ESRL PSD, Boulder, Colorado, USA, from their Web site at <https://www.esrl.noaa.gov/psd/>. SMAP soil moisture data was downloaded from NSIDC ( O'Neill, P. E., S. Chan, E. G. Njoku, T. Jackson, and R. Bindlish. 2016. SMAP L3 Radiometer Global Daily 36 km EASE-Grid Soil Moisture, Version 4. Boulder, Colorado USA. NASA National Snow and Ice Data Center Distributed Active Archive Center. doi: <https://doi.org/10.5067/OBBHQ5W22HME> [23.05.2018]). In addition, we want to thank Robin van
- 15 der Schalie for providing the AMSR2 LPRMv06 soil moisture data and Sebastian Hahn for providing the modified version of the H111 soil moisture product.

## References

- Allan, R. P. and Soden, B. J.: Atmospheric warming and the amplification of precipitation extremes, *Science*, 321, 1481–1484, 2008.
- Ambika, A. K., Wardlow, B., and Mishra, V.: Remotely sensed high resolution irrigated area mapping in India for 2000 to 2015, *Scientific data*, 3, 160 118, 2016.
- 5 Bastiaanssen, W. G., Menenti, M., Feddes, R., and Holtslag, A.: A remote sensing surface energy balance algorithm for land (SEBAL). 1. Formulation, *Journal of hydrology*, 212, 198–212, 1998.
- Bauer-Marschallinger, B., Paulik, C., Hochstöger, S., Mistelbauer, T., Modanesi, S., Ciabatta, L., Massari, C., Brocca, L., and Wagner, W.: Soil Moisture from Fusion of Scatterometer and SAR: Closing the Scale Gap with Temporal Filtering, *Remote Sensing*, 10, 2018.
- Bonfils, C. and Lobell, D.: Empirical evidence for a recent slowdown in irrigation-induced cooling, *Proceedings of the National Academy of Sciences*, 104, 13 582–13 587, 2007.
- 10 Bontemps, S., Defourny, P., Radoux, J., Van Bogaert, E., Lamarche, C., Achard, F., Mayaux, P., Boettcher, M., Brockmann, C., Kirches, G., et al.: Consistent global land cover maps for climate modelling communities: current achievements of the ESA's land cover CCI, in: *Proceedings of the ESA Living Planet Symposium*, Edimburgh, pp. 9–13, 2013.
- Bosilovich, M., Lucchesi, R., and Suarez, M.: MERRA-2: file specification, 2015.
- 15 Boucher, O., Myhre, G., and Myhre, A.: Direct human influence of irrigation on atmospheric water vapour and climate, *Climate Dynamics*, 22, 597–603, 2004.
- Brocca, L., Melone, F., Moramarco, T., Wagner, W., and Albergel, C.: Scaling and filtering approaches for the use of satellite soil moisture observations, in: *Remote Sensing of Energy Fluxes and Soil Moisture Content*, pp. 415–430, CRC Press Boca Raton, 2013.
- Chan, S., Bindlish, R., O'Neill, P., Jackson, T., Njoku, E., Dunbar, S., Chaubell, J., Piepmeier, J., Yueh, S., Entekhabi, D., et al.: Development and assessment of the SMAP enhanced passive soil moisture product, *Remote Sensing of Environment*, 204, 931–941, 2018.
- 20 Chen, M., Shi, W., Xie, P., Silva, V., Kousky, V. E., Wayne Higgins, R., and Janowiak, J. E.: Assessing objective techniques for gauge-based analyses of global daily precipitation, *Journal of Geophysical Research: Atmospheres*, 113, 2008.
- Chew, C. and Small, E.: Soil moisture sensing using spaceborne GNSS reflections: Comparison of CYGNSS reflectivity to SMAP soil moisture, *Geophysical Research Letters*, 2018.
- 25 Colliander, A., Jackson, T. J., Bindlish, R., Chan, S., Das, N., Kim, S., Cosh, M., Dunbar, R., Dang, L., Pashaian, L., et al.: Validation of SMAP surface soil moisture products with core validation sites, *Remote sensing of environment*, 191, 215–231, 2017.
- Daughtry, C., Ranson, K., and Biehl, L.: C-band backscattering from corn canopies, *International Journal of Remote Sensing*, 12, 1097–1109, 1991.
- Deines, J. M., Kendall, A. D., and Hyndman, D. W.: Annual Irrigation Dynamics in the US Northern High Plains Derived from Landsat 30 Satellite Data, *Geophysical Research Letters*, 44, 9350–9360, 2017.
- der Schalie, R., Kerr, Y., Wigneron, J., Rodr guez-Fern ndez, N., Al-Yaari, A., and Jeu, R.: Global SMOS Soil Moisture Retrievals from The Land Parameter Retrieval Model, *International Journal of Applied Earth Observation and Geoinformation*, 45, 125 – 134, <https://doi.org/https://doi.org/10.1016/j.jag.2015.08.005>, <http://www.sciencedirect.com/science/article/pii/S0303243415300179>, advances in the Validation and Application of Remotely Sensed Soil Moisture - Part 1, 2016.
- 35 D ll, P.: Impact of climate change and variability on irrigation requirements: a global perspective, *Climatic change*, 54, 269–293, 2002.
- D ll, P. and Siebert, S.: Global modeling of irrigation water requirements, *Water Resources Research*, 38, 2002.

- Dorigo, W., Xaver, A., Vreugdenhil, M., Gruber, A., Hegyiova, A., Sanchis-Dufau, A., Zamojski, D., Cordes, C., Wagner, W., and Drusch, M.: Global automated quality control of in situ soil moisture data from the International Soil Moisture Network, *Vadose Zone Journal*, 12, 2013.
- Dorigo, W., Wagner, W., Albergel, C., Albrecht, F., Balsamo, G., Brocca, L., Chung, D., Ertl, M., Forkel, M., Gruber, A., Haas, E., Hamer, P. D., Hirschi, M., Ikonen, J., de Jeu, R., Kidd, R., Lahoz, W., Liu, Y. Y., Miralles, D., Mistelbauer, T., Nicolai-Shaw, N., Parinussa, R., Pratola, C., Reimer, C., van der Schalie, R., Seneviratne, S. I., Smolander, T., and Lecomte, P.: ESA CCI Soil Moisture for improved Earth system understanding: State-of-the art and future directions, *Remote Sensing of Environment*, 203, 185 – 215, <https://doi.org/https://doi.org/10.1016/j.rse.2017.07.001>, <http://www.sciencedirect.com/science/article/pii/S0034425717303061>, *Earth Observation of Essential Climate Variables*, 2017.
- 10 Entekhabi, D., Njoku, E. G., O'Neill, P. E., Kellogg, K. H., Crow, W. T., Edelstein, W. N., Entin, J. K., Goodman, S. D., Jackson, T. J., Johnson, J., et al.: The soil moisture active passive (SMAP) mission, *Proceedings of the IEEE*, 98, 704–716, 2010.
- Escorihuela, M. J. and Quintana-Seguí, P.: Comparison of remote sensing and simulated soil moisture datasets in Mediterranean landscapes, *Remote sensing of environment*, 180, 99–114, 2016.
- Foley, J. A., Ramankutty, N., Brauman, K. A., Cassidy, E. S., Gerber, J. S., Johnston, M., Mueller, N. D., O'Connell, C., Ray, D. K., West, P. C., et al.: Solutions for a cultivated planet, *Nature*, 478, 337, 2011.
- Hahn, S., Reimer, C., Vreugdenhil, M., Melzer, T., and Wagner, W.: Dynamic characterization of the incidence angle dependence of backscatter using metop ASCAT, *IEEE Journal of Selected Topics in Applied Earth Observations and Remote Sensing*, 10, 2348–2359, 2017.
- Hain, C. R., Crow, W. T., Anderson, M. C., and Yilmaz, M. T.: Diagnosing neglected soil moisture source–sink processes via a thermal infrared–based two-source energy balance model, *Journal of Hydrometeorology*, 16, 1070–1086, 2015.
- 20 Howitt, R.: Preliminary Analysis: 2015 Drought Economic Impact Study, Tech. rep., California Department of Food and Agriculture, 2015.
- Imaoka, K., Kachi, M., Fujii, H., Murakami, H., Hori, M., Ono, A., Igarashi, T., Nakagawa, K., Oki, T., Honda, Y., et al.: Global Change Observation Mission (GCOM) for monitoring carbon, water cycles, and climate change, *Proceedings of the IEEE*, 98, 717–734, 2010.
- Joseph, A., van der Velde, R., O'Neill, P., Lang, R., and Gish, T.: Effects of corn on C- and L-band radar backscatter: A correction method for soil moisture retrieval, *Remote Sensing of Environment*, 114, 2417–2430, 2010.
- 25 Kebede, H., Fisher, D. K., Sui, R., Reddy, K. N., et al.: Irrigation methods and scheduling in the delta region of Mississippi: Current status and strategies to improve irrigation efficiency, *American Journal of Plant Sciences*, 5, 2917, 2014.
- Kottek, M., Grieser, J., Beck, C., Rudolf, B., and Rubel, F.: World map of the Köppen-Geiger climate classification updated, *Meteorologische Zeitschrift*, 15, 259–263, 2006.
- Kueppers, L. M., Snyder, M. A., and Sloan, L. C.: Irrigation cooling effect: Regional climate forcing by land-use change, *Geophysical Research Letters*, 34, 2007.
- 30 Kumar, S. V., Peters-Lidard, C. D., Santanello, J. A., Reichle, R. H., Draper, C. S., Koster, R. D., Nearing, G., and Jasinski, M. F.: Evaluating the utility of satellite soil moisture retrievals over irrigated areas and the ability of land data assimilation methods to correct for unmodeled processes, *Hydrology and Earth System Sciences*, 19, 4463–4478, <https://doi.org/10.5194/hess-19-4463-2015>, <http://dx.doi.org/10.5194/hess-19-4463-2015>, 2015.
- 35 Kumar, S. V., JASINSKI, M., MOCKO, D., RODELL, M., BORAK, J., LI, B., KATO BEAUDOING, H., and PETERS-LIDARD, C. D.: NCA-LDAS land analysis: Development and performance of a multisensor, multivariate land data assimilation system for the National Climate Assessment, *Journal of Hydrometeorology*, 2018.



- Kummu, M., Guillaume, J., De Moel, H., Eisner, S., Flörke, M., Porkka, M., Siebert, S., Veldkamp, T., and Ward, P.: The world's road to water scarcity: shortage and stress in the 20th century and pathways towards sustainability, *Scientific reports*, 6, 38495, 2016.
- Lawston, P. M., Santanello Jr, J. A., Zaitchik, B. F., and Rodell, M.: Impact of irrigation methods on land surface model spinup and initialization of WRF forecasts, *Journal of Hydrometeorology*, 16, 1135–1154, 2015.
- 5 Lawston, P. M., Santanello, J. A., and Kumar, S. V.: Irrigation Signals Detected From SMAP Soil Moisture Retrievals, *Geophysical Research Letters*, 2017.
- Linguist, B., Snyder, R., Anderson, F., Espino, L., Inglese, G., Marras, S., Moratiel, R., Mutters, R., Nicolosi, P., Rejmanek, H., et al.: Water balances and evapotranspiration in water-and dry-seeded rice systems, *Irrigation science*, 33, 375–385, 2015.
- Liu, Y. Y., Dorigo, W. A., Parinussa, R., de Jeu, R. A., Wagner, W., McCabe, M. F., Evans, J., and Van Dijk, A.: Trend-preserving blending of passive and active microwave soil moisture retrievals, *Remote Sensing of Environment*, 123, 280–297, 2012.
- 10 Lobell, D. B., Bala, G., and Duffy, P. B.: Biogeophysical impacts of cropland management changes on climate, *Geophysical Research Letters*, 33, n/a–n/a, <https://doi.org/10.1029/2005GL025492>, <http://dx.doi.org/10.1029/2005GL025492>, 106708, 2006.
- Loveland, T. R., Reed, B. C., Brown, J. F., Ohlen, D. O., Zhu, Z., Yang, L., and Merchant, J. W.: Development of a global land cover characteristics database and IGBP DISCover from 1 km AVHRR data, *International Journal of Remote Sensing*, 21, 1303–1330, 2000.
- 15 Masson, V., Le Moigne, P., Martin, E., Faroux, S., Alias, A., Alkama, R., Belamari, S., Barbu, A., Boone, A., Bouysse, F., et al.: The SURFEXv7. 2 land and ocean surface platform for coupled or offline simulation of earth surface variables and fluxes, *Geoscientific Model Development*, 6, 929–960, 2013.
- McColl, K. A., Alemohammad, S. H., Akbar, R., Konings, A. G., Yueh, S., and Entekhabi, D.: The global distribution and dynamics of surface soil moisture, *Nature Geoscience*, 10, 100–104, <https://doi.org/10.1038/ngeo2868>, <http://dx.doi.org/10.1038/NGEO2868>, 2017.
- 20 Meier, J., Zabel, F., and Mauser, W.: A global approach to estimate irrigated areas—a comparison between different data and statistics, *Hydrology and Earth System Sciences*, 22, 1119–1133, 2018.
- Naeimi, V., Scipal, K., Bartalis, Z., Hasenauer, S., and Wagner, W.: An improved soil moisture retrieval algorithm for ERS and METOP scatterometer observations, *IEEE Transactions on Geoscience and Remote Sensing*, 47, 1999–2013, 2009.
- NASS, U.: Usual planting and harvesting dates for US field crops, Tech. rep., 2010.
- 25 NASS, U.: Census of agriculture, US Department of Agriculture, National Agricultural Statistics Service, Washington, DC, 1, 2012.
- Nguyen, D. B., Clauss, K., Cao, S., Naeimi, V., Kuenzer, C., and Wagner, W.: Mapping Rice Seasonality in the Mekong Delta with Multi-Year Envisat ASAR WSM Data, *Remote Sensing*, 7, 15868–15893, <https://doi.org/10.3390/rs71215808>, <http://www.mdpi.com/2072-4292/7/12/15808>, 2015.
- Owe, M., de Jeu, R., and Holmes, T.: Multisensor historical climatology of satellite-derived global land surface moisture, *Journal of Geophysical Research: Earth Surface*, 113, 2008.
- 30 Ozdogan, M. and Gutman, G.: A new methodology to map irrigated areas using multi-temporal MODIS and ancillary data: An application example in the continental US, *Remote Sensing of Environment*, 112, 3520–3537, <https://doi.org/10.1016/j.rse.2008.04.010>, <http://dx.doi.org/10.1016/j.rse.2008.04.010>, 2008.
- Ozdogan, M., Woodcock, C. E., Salvucci, G. D., and Demir, H.: Changes in summer irrigated crop area and water use in Southeastern Turkey from 1993 to 2002: Implications for current and future water resources, *Water resources management*, 20, 467–488, 2006.
- 35 Ozdogan, M., Rodell, M., Beaudoin, H. K., and Toll, D. L.: Simulating the Effects of Irrigation over the United States in a Land Surface Model Based on Satellite-Derived Agricultural Data, *Journal of Hydrometeorology*, 11, 171–184, <https://doi.org/10.1175/2009jhm1116.1>, <http://dx.doi.org/10.1175/2009JHM1116.1>, 2010a.

- Ozdogan, M., Yang, Y., Allez, G., and Cervantes, C.: Remote Sensing of Irrigated Agriculture: Opportunities and Challenges, *Remote Sensing*, 2, 2274–2304, <https://doi.org/10.3390/rs2092274>, <http://dx.doi.org/10.3390/rs2092274>, 2010b.
- Pereira, L. S., Oweis, T., and Zairi, A.: Irrigation management under water scarcity, *Agricultural water management*, 57, 175–206, 2002.
- Pervez, M. S. and Brown, J. F.: Mapping Irrigated Lands at 250-m Scale by Merging MODIS Data and National Agricultural Statistics, *Remote Sensing*, 2, 2388–2412, <https://doi.org/10.3390/rs2102388>, <http://dx.doi.org/10.3390/rs2102388>, 2010.
- Pervez, S., Brown, J. F., and Maxwell, S.: Evaluation of remote sensing-based irrigated area map for the Conterminous United States, *Proceedings of the ASPRS Pecora*, 17, 2008.
- Portmann, F. T., Siebert, S., and Döll, P.: MIRCA2000 - Global monthly irrigated and rainfed crop areas around the year 2000: A new high-resolution data set for agricultural and hydrological modeling, *Global biogeochemical cycles*, 24, 2010.
- Pun, M., Mutiibwa, D., and Li, R.: Land Use Classification: A Surface Energy Balance and Vegetation Index Application to Map and Monitor Irrigated Lands, *Remote Sensing*, 9, 1256, 2017.
- Qiu, J., Gao, Q., Wang, S., and Su, Z.: Comparison of temporal trends from multiple soil moisture data sets and precipitation: The implication of irrigation on regional soil moisture trend, *International journal of applied earth observation and geoinformation*, 48, 17–27, 2016.
- Reichle, R. H., Draper, C. S., Liu, Q., Giroto, M., Mahanama, S. P., Koster, R. D., and De Lannoy, G. J.: Assessment of MERRA-2 land surface hydrology estimates, *Journal of Climate*, 30, 2937–2960, <https://journals.ametsoc.org/doi/abs/10.1175/JCLI-D-16-0720.1>, 2017a.
- Reichle, R. H., Liu, Q., Koster, R. D., Draper, C. S., Mahanama, S. P., and Partyka, G. S.: Land surface precipitation in MERRA-2, *Journal of Climate*, 30, 1643–1664, <https://doi.org/https://doi.org/10.1175/JCLI-D-16-0570.1>, <https://journals.ametsoc.org/doi/abs/10.1175/JCLI-D-16-0570.1>, 2017b.
- Rockström, J., Falkenmark, M., Lannerstad, M., and Karlberg, L.: The planetary water drama: Dual task of feeding humanity and curbing climate change, *Geophysical Research Letters*, 39, 2012.
- Rosas, J., Houborg, R., and McCabe, M. F.: Sensitivity of Landsat 8 Surface Temperature Estimates to Atmospheric Profile Data: A Study Using MODTRAN in Dryland Irrigated Systems, *Remote Sensing*, 9, 988, 2017.
- Roseta-Palma, C., Iglesias, E., and Koppl-Turyna, M.: Illegal groundwater pumping, in: 5th World Congress of Environmental and Resource Economists, Istanbul, Turkey, paper, vol. 863, 2014.
- Sacks, W. J., Cook, B. I., Buening, N., Levis, S., and Helkowski, J. H.: Effects of global irrigation on the near-surface climate, *Climate Dynamics*, 33, 159–175, <https://doi.org/10.1007/s00382-008-0445-z>, <http://dx.doi.org/10.1007/s00382-008-0445-z>, 2009.
- Saffi, M. and Cheddadi, A.: Identification of illegal groundwater pumping in semi-confined aquifers, *Hydrological Sciences Journal–Journal des Sciences Hydrologiques*, 55, 1348–1356, 2010.
- Salmon, J. M., Friedl, M. A., Frohling, S., Wisser, D., and Douglas, E. M.: Global rain-fed, irrigated, and paddy croplands: A new high resolution map derived from remote sensing, crop inventories and climate data, *International Journal of Applied Earth Observation and Geoinformation*, 38, 321–334, 2015.
- Seneviratne, S. I., Corti, T., Davin, E. L., Hirschi, M., Jaeger, E. B., Lehner, I., Orlowsky, B., and Teuling, A. J.: Investigating soil moisture–climate interactions in a changing climate: A review, *Earth-Science Reviews*, 99, 125 – 161, <https://doi.org/https://doi.org/10.1016/j.earscirev.2010.02.004>, <http://www.sciencedirect.com/science/article/pii/S0012825210000139>, 2010.
- Shiklomanov, I. A.: Appraisal and assessment of world water resources, *Water international*, 25, 11–32, 2000.

- Siebert, S., Döll, P., Hoogeveen, J., Faures, J.-M., Frenken, K., and Feick, S.: Development and validation of the global map of irrigation areas, *Hydrology and Earth System Sciences*, 9, 535–547, <https://doi.org/10.5194/hess-9-535-2005>, <http://www.hydrol-earth-syst-sci.net/9/535/2005/>, 2005.
- Siebert, S., Döll, P., Feick, S., Hoogeveen, J., and Frenken, K.: Global map of irrigation areas version 4.0. 1, Johann Wolfgang Goethe University, Frankfurt am Main, Germany/Food and Agriculture Organization of the United Nations, Rome, Italy, 2007.
- Siebert, S., Burke, J., Faures, J. M., Frenken, K., Hoogeveen, J., Döll, P., and Portmann, F. T.: Groundwater use for irrigation - a global inventory, *Hydrology and Earth System Sciences*, 14, 1863–1880, <https://doi.org/10.5194/hess-14-1863-2010>, <https://www.hydrol-earth-syst-sci.net/14/1863/2010/>, 2010.
- Siebert, S., Kumm, M., Porkka, M., Döll, P., Ramankutty, N., and Scanlon, B. R.: A global data set of the extent of irrigated land from 1900 to 2005, *Hydrology and Earth System Sciences*, 19, 1521–1545, 2015.
- Taylor, R. G., Scanlon, B., Döll, P., Rodell, M., van Beek, R., Wada, Y., Longuevergne, L., Leblanc, M., Famiglietti, J. S., Edmunds, M., and et al.: Ground water and climate change, *Nature Climate Change*, 3, 322–329, <https://doi.org/10.1038/nclimate1744>, <http://dx.doi.org/10.1038/NCLIMATE1744>, 2012.
- Teluguntla, P., Thenkabail, P. S., Xiong, J., Gumma, M. K., Congalton, R. G., Oliphant, A., Poehnelt, J., Yadav, K., Rao, M., and Massey, R.: Spectral matching techniques (SMTs) and automated cropland classification algorithms (ACCAs) for mapping croplands of Australia using MODIS 250-m time-series (2000-2015) data, *International Journal of Digital Earth*, 10, 944–977, 2017.
- Thenkabail, P. S., Biradar, C. M., Noojipady, P., Dheeravath, V., Li, Y., Velpuri, M., Gumma, M., Gangalakunta, O. R. P., Turrall, H., Cai, X., et al.: Global irrigated area map (GIAM), derived from remote sensing, for the end of the last millennium, *International Journal of Remote Sensing*, 30, 3679–3733, 2009.
- Thiery, W., Davin, E. L., Lawrence, D. M., Hirsch, A. L., Hauser, M., and Seneviratne, S. I.: Present-day irrigation mitigates heat extremes, *Journal of Geophysical Research: Atmospheres*, 122, 1403–1422, 2017.
- Tuinenburg, O. and Vries, J.: Irrigation Patterns Resemble ERA-Interim Reanalysis Soil Moisture Additions, *Geophysical Research Letters*, 44, 2017.
- USDA: Farm and Ranch Irrigation Survey, Tech. rep., United States Department of Agriculture, 2013.
- Vörösmarty, C. J., Green, P., Salisbury, J., and Lammers, R. B.: Global water resources: vulnerability from climate change and population growth, *science*, 289, 284–288, 2000.
- Vreugdenhil, M., Dorigo, W. A., Wagner, W., De Jeu, R. A., Hahn, S., and Van Marle, M. J.: Analyzing the vegetation parameterization in the TU-Wien ASCAT soil moisture retrieval, *IEEE Transactions on Geoscience and Remote Sensing*, 54, 3513–3531, 2016.
- Wagner, W., Lemoine, G., and Rott, H.: A method for estimating soil moisture from ERS scatterometer and soil data, *Remote sensing of environment*, 70, 191–207, 1999.
- Wagner, W., Hahn, S., Kidd, R., Melzer, T., Bartalis, Z., Hasenauer, S., Figa-Saldaña, J., de Rosnay, P., Jann, A., Schneider, S., et al.: The ASCAT soil moisture product: A review of its specifications, validation results, and emerging applications, *Meteorologische Zeitschrift*, 22, 5–33, 2013.
- Wei, J., Dirmeyer, P. A., Wissler, D., Bosilovich, M. G., and Mocko, D. M.: Where Does the Irrigation Water Go? An Estimate of the Contribution of Irrigation to Precipitation Using MERRA, *Journal of Hydrometeorology*, 14, 275–289, <https://doi.org/10.1175/jhm-d-12-079.1>, <http://dx.doi.org/10.1175/JHM-D-12-079.1>, 2013.
- Xie, P., Chen, M., and Shi, W.: CPC unified gauge-based analysis of global daily precipitation, in: Preprints, 24th Conf. on Hydrology, Atlanta, GA, Amer. Meteor. Soc, vol. 2, [https://ams.confex.com/ams/90annual/techprogram/paper\\_163676.htm](https://ams.confex.com/ams/90annual/techprogram/paper_163676.htm), 2010.

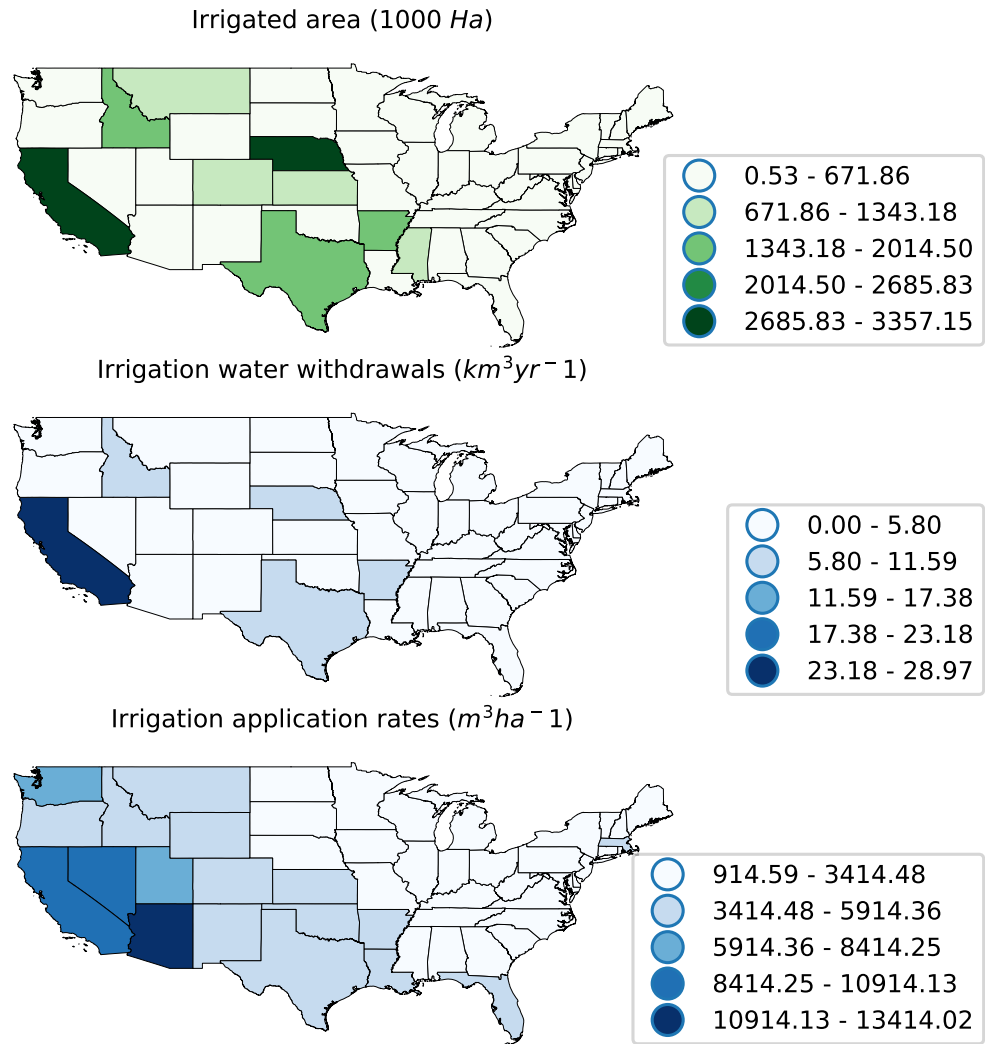


**Figure 1. Per-state irrigated area, irrigation water withdrawals, and irrigation water application rates for 2013.** The data was drawn from the latest Farm and Ranch Irrigation Survey (FRIS) and only reflects irrigation operations in open fields (e.g. excluding crops grown and irrigated in greenhouses).

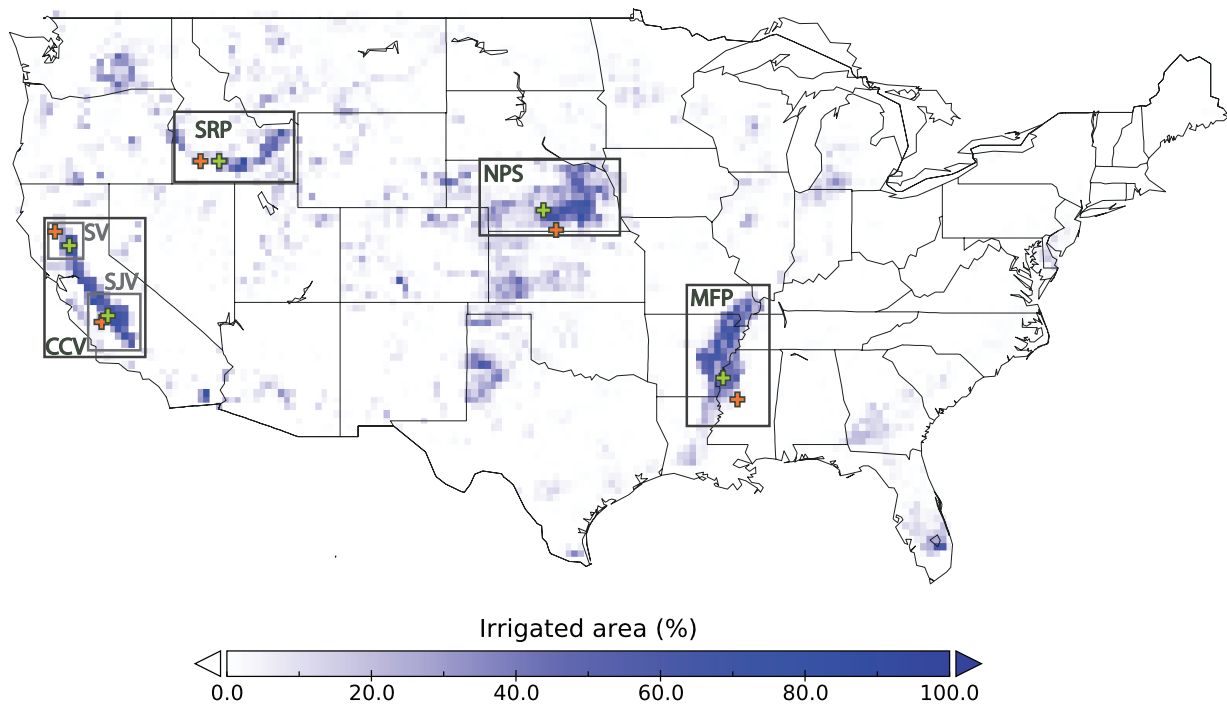


**Figure 2. Study regions and locations of the pixels selected for a local time series analysis over the fractional irrigated area map derived from the spatially aggregated M<sub>ir</sub>AD-US data set (Pervez and Brown, 2010). The focus regions are included in black squares and include: the Sacramento Valley (SV) and San Joaquin Valley (SJ) in the California Central Valley (CCV); Snake River Plain (SRP); Nebraska Plains (NPS), and the Mississippi Flood Plain (MFP). Green and orange crosses indicate the locations of the irrigated (P-I) and non-irrigated (P-NI) pixels, respectively, at which we further analyze satellite and model soil moisture time series in conjunction with  $\overline{TWU}$  estimates.**

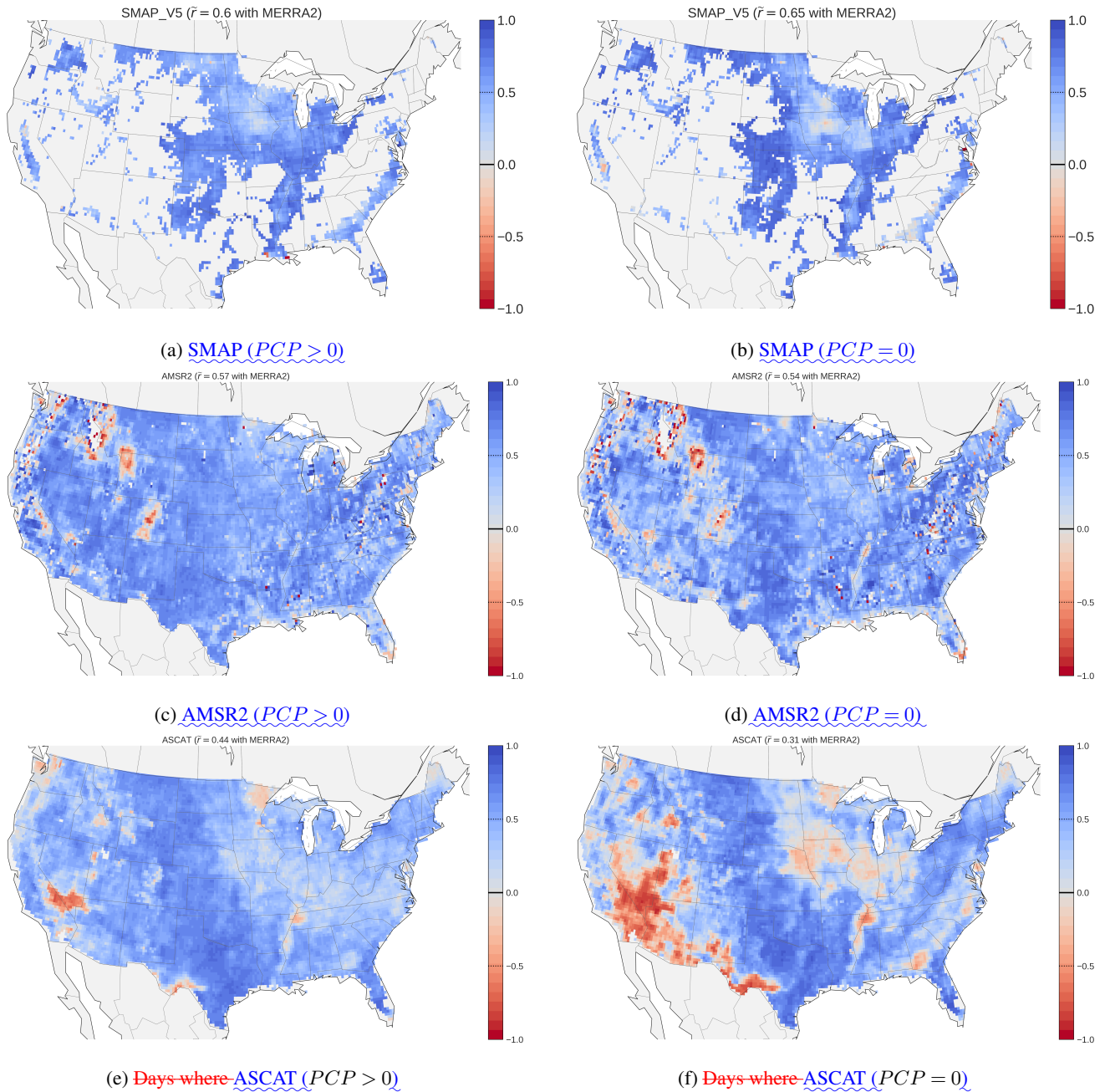


**Figure 3. Mean correlation  $\bar{r}$  between the daily time series of each satellite soil moisture product (SMAP, AMSR2 and ASCAT) and MERRA-2 soil moisture separated for dry periods (first column; precipitation  $PCP > 0$ ) and dry periods (second column;  $PCP = 0$ ) during the growing season. Correlations were calculated over agricultural areas only.** Mean correlation  $\bar{r}$  between the daily time series of each satellite soil moisture product (SMAP, AMSR2 and ASCAT) and MERRA-2 soil moisture separated for wet periods (first column; precipitation  $PCP > 0$ ) and dry periods (second column;  $PCP = 0$ ) during the growing season. Correlations were calculated over agricultural areas only.

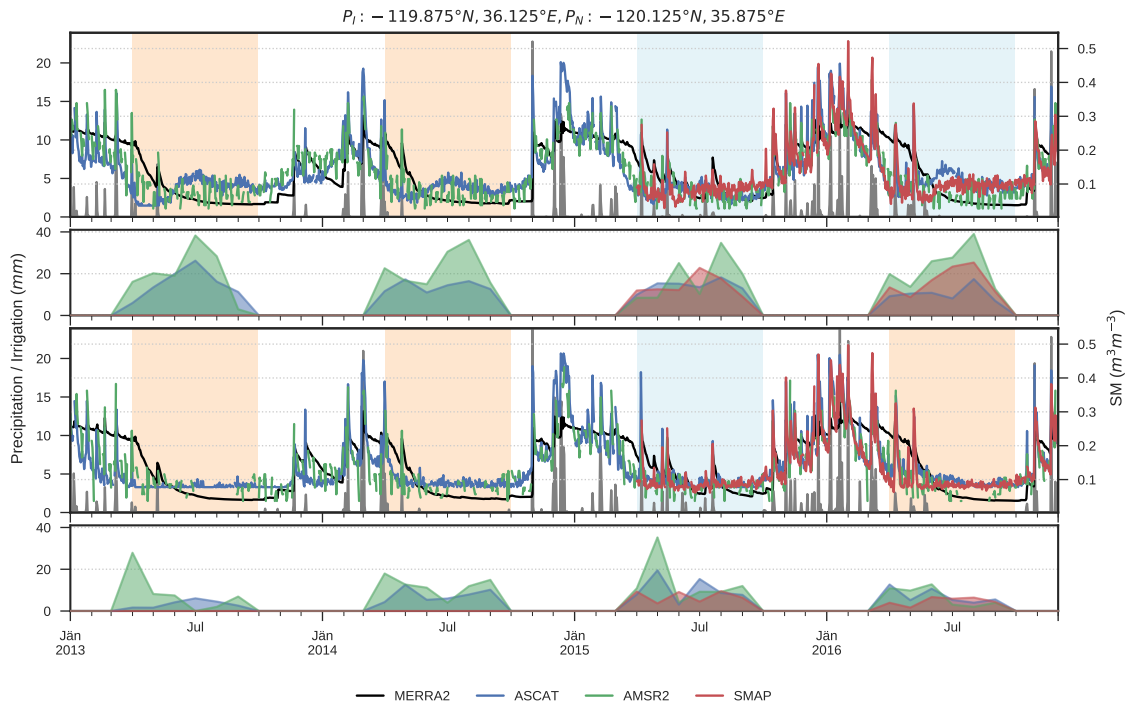
(a) SMAP

(b) AMSR2

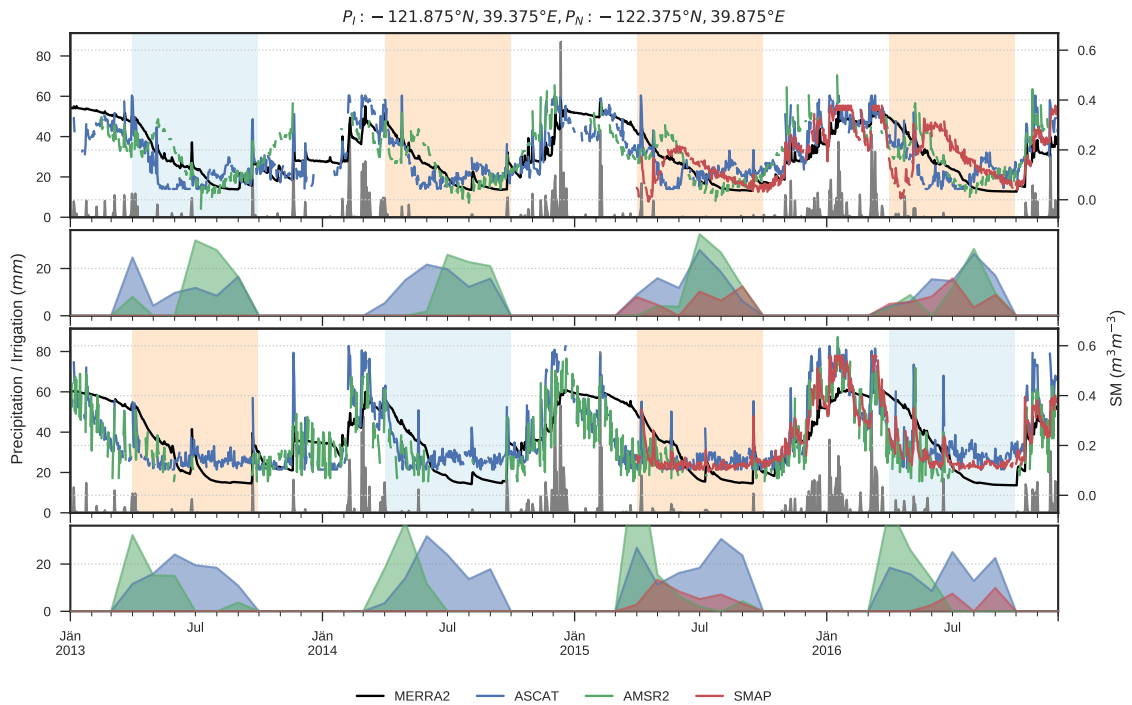
(c) ASCAT

**Figure 4. Mean annual irrigation water use  $\overline{IWU}_A$  derived from SMAP (4a), AMSR2 (4b) and ASCAT SM (4c) in combination with modeled SM from MERRA-2. Mean annual irrigation water use  $\overline{IWU}_A$  derived from SMAP- (4a), AMSR2- (4b) and ASCAT-SM (4c) in combination with modeled SM from MERRA-2.** All pixels with a cropland fraction of < 5% (as inferred from the CCI land cover product) were excluded from the analysis. Note that for SMAP the climatologies represent the growing season mean of 2015 and 2016, while for AMSR2 and ASCAT the estimates are derived from 4 years of data covering the period of 2013-2016. **The upper limit of the colorbar is fixed at the 99th percentile of the SMAP-based estimates.**

(a) San Joaquin Valley, California

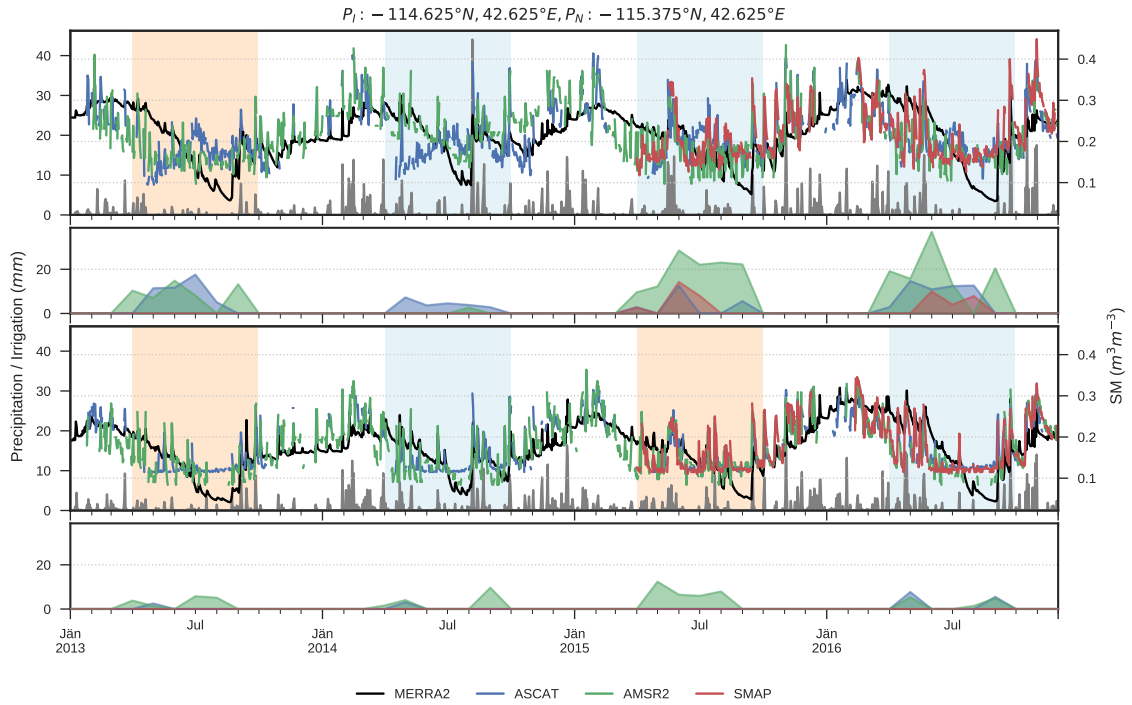


(b) Sacramento Valley, California

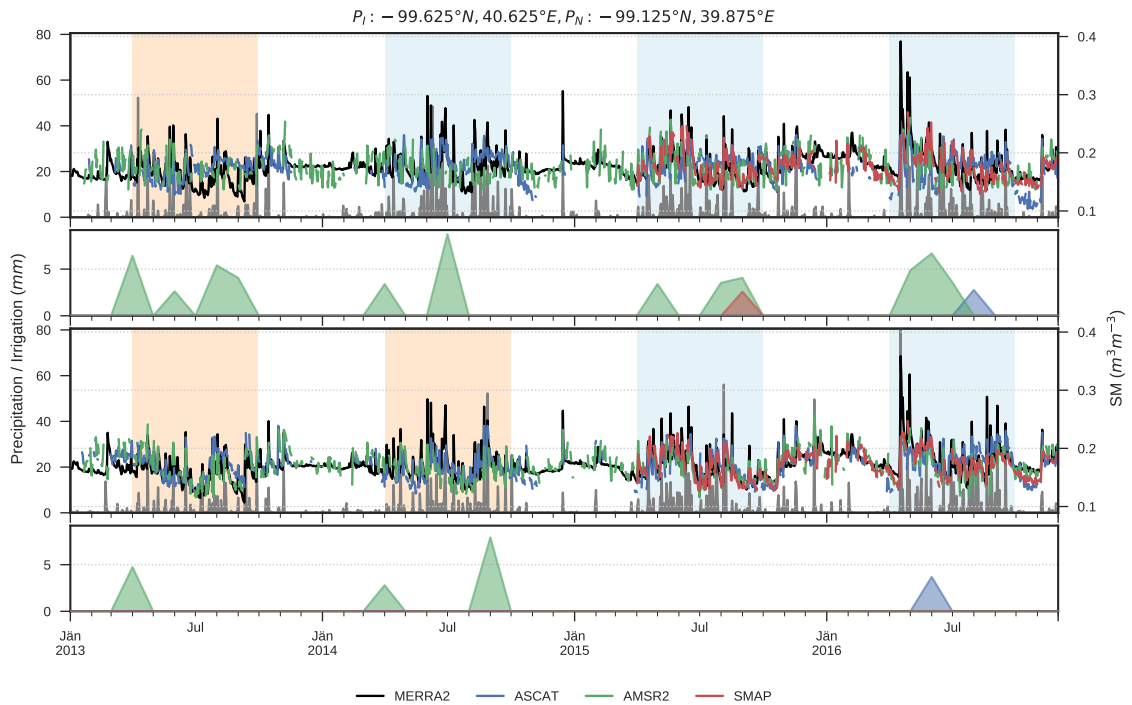




(c) Snake River Plain, Idaho



(d) High Plains, Nebraska



(e) Lower Mississippi Floodplain, Mississippi

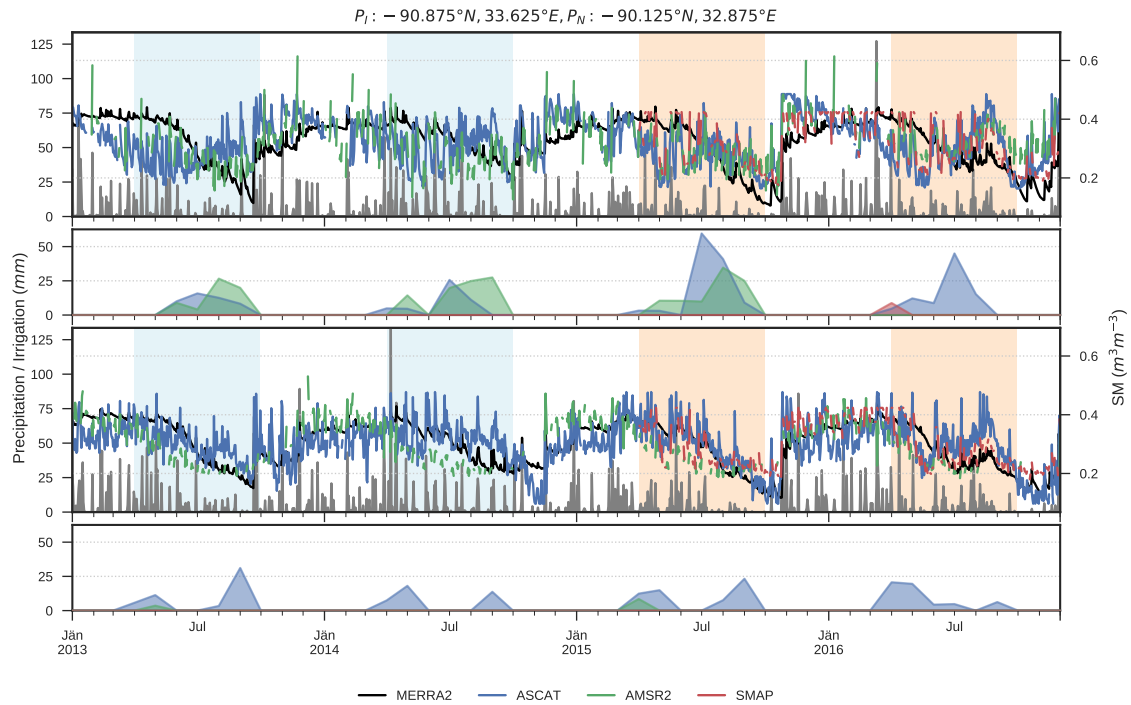


**Figure 5. (continued) Comparison of satellite and model SM time series at irrigated (top two sub-panels) and non-irrigated pixels (bottom two sub-panels) in four regions (figures 5a - 5e).** Daily CPC precipitation is plotted in grey, while blue and orange shadings in the top sub-panels reflect growing seasons with positive and negative rainfall anomalies respectively. The bottom sub-panels show the estimated monthly irrigation water use ( $\overline{IWU}_M$ ) obtained for each satellite-model pair (non-growing season periods have been masked).

**Figure 6. Comparison of estimated mean annual irrigation water use and reported irrigation water withdrawals.** For each satellite-model pair, observed  $\overline{IWU}_A$  was aggregated at the state level. Reported irrigation withdrawals were taken from the 2013 FRIS report and only reflect volumes applied in open fields (e.g. excluding crops grown and irrigated in greenhouses). The data are presented in logarithmic units to reflect both small and large water volumes. Note that the names of the 10 states accounting for the highest irrigation water withdrawals are annotated.  $R$ ,  $RMSE$  and  $bias$  between observed and reported estimates are shown in the bottom right of each subplot.

**Table 1.** Data products

<b>Data</b>	<b>Product name</b>	<b>Data availability/ Reference time</b>	<b>Temporal resolution</b>	<b>Spatial resolution</b>	<b>Native gridding</b>	<b>Units</b>
SMAP	SMAP_L3_v4	04/2015 - present	1-3 days	~40 km	36 km	$\text{cm}^3 \text{cm}^{-3}$
AMSR2	LPRM v06	07/2012 - present	1-2 days	~25 km	$0.25^\circ$	$\text{m}^3 \text{m}^{-3}$
ASCAT	modified H111	01/2007 - present	~1.5 days	~25 km	12.5 km	%
MERRA-2	M2T1NXLND.5.12.4 (SFMC parameter)	01/1980 - present	1 day (resampled)	~50 km	$0.625^\circ \times 0.5^\circ$	$\text{m}^3 \text{m}^{-3}$
ESA CCI Land Cover	LC map 2010 epoch	2008-2012	-	$0.25^\circ$ (resampled)	300 m	-
CPC Precipitation	Unified Gauge-Based Analysis of Daily Precipitation	01/2007 - 12/2016	1 day	$0.25^\circ$	$0.25^\circ$	mm/day
MIrAD-US	MODIS Irrigated Agriculture Dataset for the United States v3	2012	-	$0.25^\circ$ (resampled)	250 m	-

**Table 2. Accuracy assessment of irrigated area estimates.** For each satellite-model combination a confusion matrix between observed  $\overline{IWU}_A$  and reference irrigated area from the spatially aggregated 2012 MirAD-US data set was computed after converting the continuous data to a binary representation. Specifically, pixels with observed  $\overline{IWU}_A \geq 20\text{mm}$  and reported  $A_{irrigated} \geq 5\%$  were respectively assigned to the irrigated classes. The binarisation thresholds  $X$  were found by maximizing the respective kappa scores for each satellite-model combination within each region (see figure A5). Results are shown for the four states selected in the regional analysis and the contiguous-US (whole CONUS). Underlines indicate the best scores within each region, while bold scores show the overall best.

Region	Satellite-SM product	Error-of-omission-X (%mm)	Error-of-comission-EoO (%)	Overall-accuracy-EoC (%)	Kappa-score
California	SMAP	<u>4.946</u>	<u>21.43</u> <b>2.47</b>	<u>23.30</u>	<b>77.68</b> <u>76.79</u>
	AMSR2	<del>12.35</del> <u>20</u>	<del>26.04</del> <u>17.28</u>	<u>23.86</u>	68.75
	ASCAT	<u>21</u>	<u>7.41</u>	<u>4.94</u> <u>22.68</u>	<del>24.51</del> <u>75.00</u>
Idaho	SMAP	<u>90.16</u> <u>4</u>	<del>45.45</del> <u>44.26</u>	<del>50.82</del> <u>45.16</u>	<del>0.02</del> <u>54.92</u>
	AMSR2	<u>9</u>	<del>40.98</del> <u>36.07</u>	<del>40.98</del> <u>40.91</u>	<del>59.02</del> <u>59.84</u>
	ASCAT	<del>77.05</del> <u>7</u>	<del>39.13</del> <u>65.57</u>	<del>54.1</del> <u>41.67</u>	<del>0.08</del> <u>54.92</u>
Nebraska	SMAP	<del>100</del> <u>0</u>	<del>68.88</del>	<del>19.01</del> <u>17.57</u>	<del>0</del> <u>38.84</u>
	AMSR2	<u>3</u>	<u>35.71</u>	<del>95.92</del> <b>15.44</b>	<del>42.86</del> <u>61.57</u>
	ASCAT	<del>99.49</del> <u>2</u>	<del>50</del> <u>23.47</u>	<del>19.01</del> <u>18.48</u>	<del>-0.01</del> <u>66.94</u>
Mississippi	SMAP	<u>12</u>	100	100	<del>60</del> <u>64.44</u>
	AMSR2	<del>54.84</del> <u>6</u>	<del>39.13</del> <u>35.48</u>	<del>71.11</del> <u>44.44</u>	<u>0.32</u> <u>70</u>
	ASCAT	<u>21</u>	<b>06.45</b>	<del>62.65</del> <u>50</u>	<del>42.22</del> <u>65.56</u>
CONUS	SMAP	<del>90.05</del> <u>8</u>	<del>53.64</del> <u>86.75</u>	<del>74.03</del> <u>58.61</u>	<del>0.08</del> <u>72.96</u>
	AMSR2	<u>5</u>	<del>72.74</del> <u>49.63</u>	<del>67.64</del> <u>68.37</u>	<del>66.82</del> <u>59.38</u>
	ASCAT	<del>74.75</del> <u>21</u>	<del>74.65</del> <u>86.09</u>	<del>61.88</del> <u>48.79</u>	<del>0</del> <u>74.55</u>

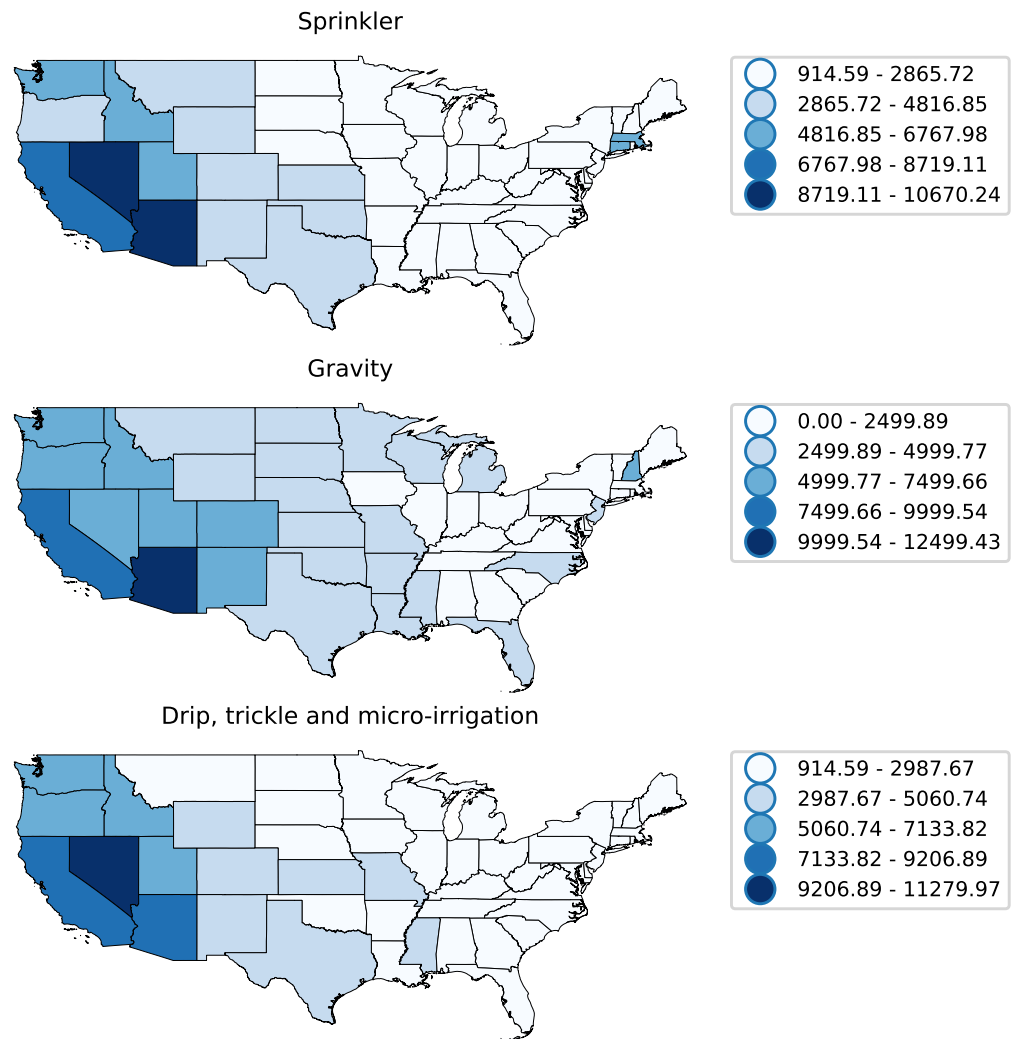
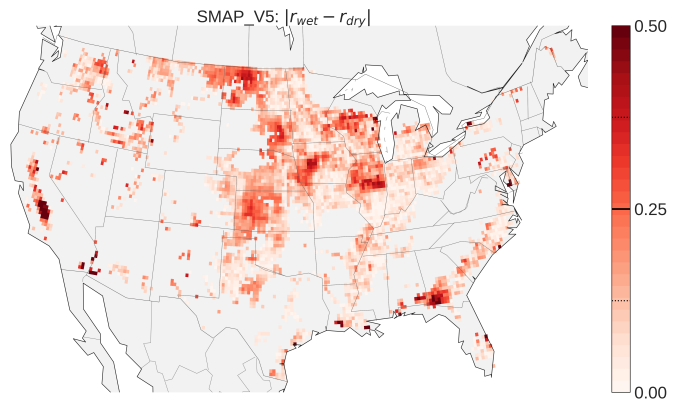
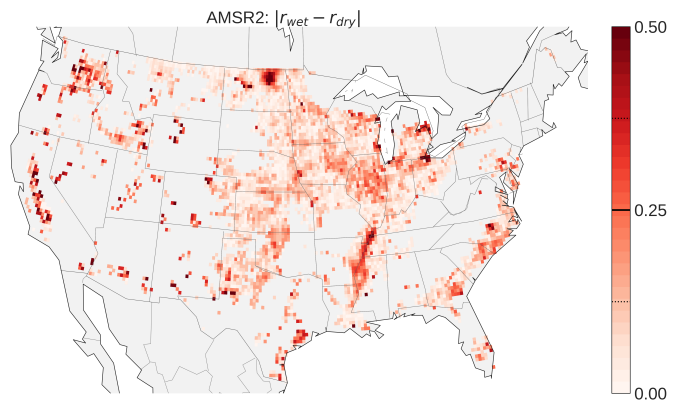


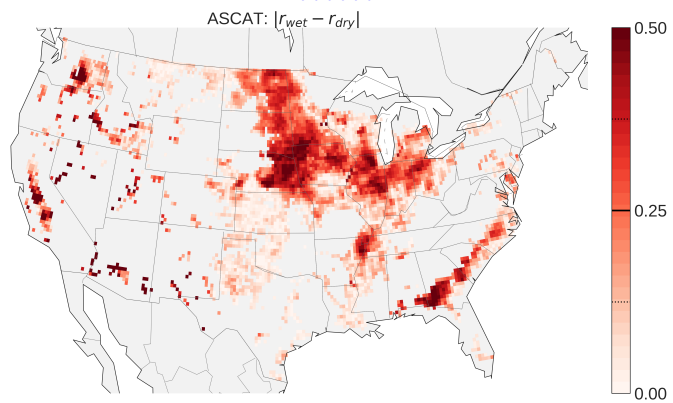
**Figure A1. Per-state irrigation water application rates ( $\text{m}^3 \text{ha}^{-1}$ ) by irrigation technique for 2013.** In accordance with figure 1, the data was derived from the 2013 FRIS and only reflects irrigation operations in open fields.



(a) SMAP



(b) AMSR2



(c) ASCAT

Figure A2. Absolute differences between the mean correlations for wet and dry periods  $|r_{wet} - r_{dry}|$ .

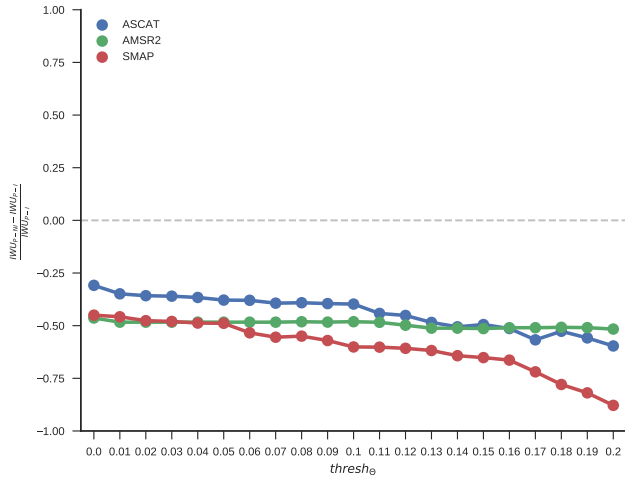
figures/methods/num\_days\_with\_iwu\_SMAP\_V5.png

(a) SMAP

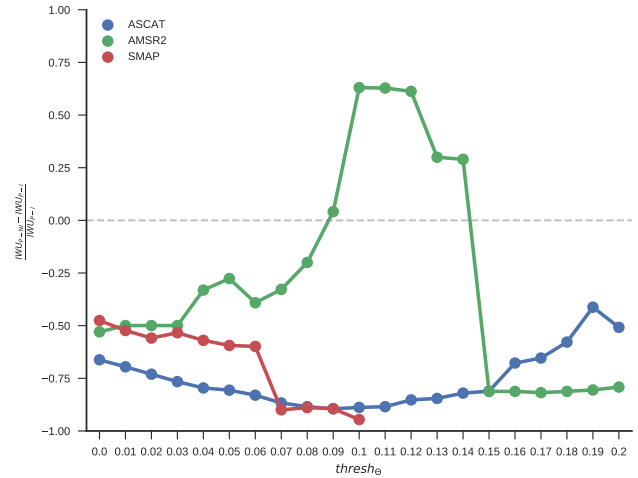
figures/methods/num\_days\_with\_iwu\_AMSR2.png

(b) AMSR2

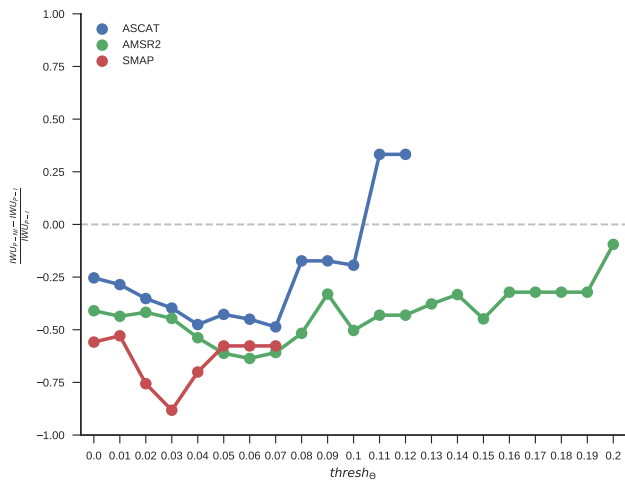




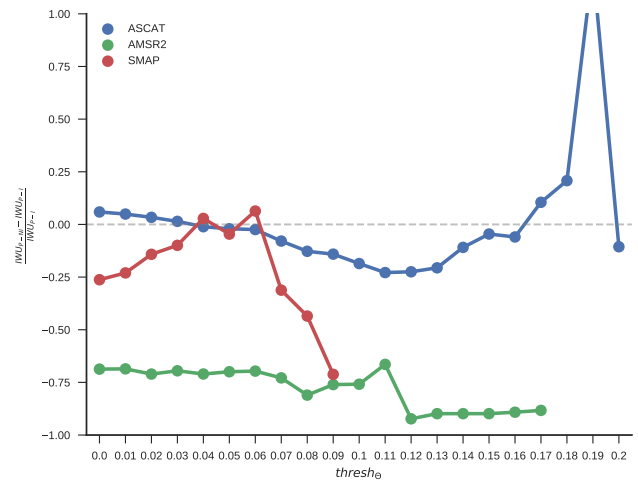
(a) San Joaquin Valley, California



(b) Snake River Plain, Idaho



(c) Nebraska plains



(d) Mississippi Flood Plain

**Figure A4. Local optimisation of the noise threshold  $thresh_{\theta}$ .** For each focus area, the relative differences in irrigation water use ( $\overline{IWU}$ ) estimated at a representative pixel covering a non-irrigated (PNI) and irrigated pixel (PI), respectively ( $\frac{IWU_{PNI} - IWU_{PI}}{IWU_{PI}}$ ) are plotted against  $thresh_{\theta}$  choices of 0 – 0.2.

figures/methods/California\_determination\_of\_threshold\_for\_binarisation\_despined.pdf

**Figure A5. Determination of the binarisation threshold  $X$ .** Accuracy metrics were calculated between a binary representation of estimated IWU and irrigated areas based on the M<sub>Ir</sub>AD-US product. Example for the state of California.

**Table A1. Sensitivity of IWU to optimisation of  $tresh_{\Theta}$  for the entire CONUS.** State-level agreement between estimated annual mean IWU and reference irrigation water withdrawals reported by the 2013 FRIS. The noise threshold  $tresh_{\Theta}$  is applied to the relative increases in satellite soil moisture  $\frac{d\Theta_{sat}}{\Theta_{sat}^{t-n}}$  in rain-free periods. Underlined performance scores indicate the best scores within each category.

Threshold	satellite	R	<del>RMSD</del> <u>RMSE</u> ( $km^3$ )	bias ( $km^3$ )
$\frac{d\Theta_{sat}}{\Theta_{sat}^{t-n}} \geq 4\%$	SMAP <u>V5</u>	<del>0.65</del> <u>0.72</u>	<del>5.09</del> <u>5.25</u>	<del>-2.26</del> <u>-2.40</u>
	AMSR2	0.35	<del>4.95</del> <u>5.17</u>	<del>-1.85</del> <u>-2.19</u>
	ASCAT	0.15	<del>4.99</del> <u>5.15</u>	<del>-1.48</del> <u>-2.01</u>
$\frac{d\Theta_{sat}}{\Theta_{sat}^{t-n}} \geq 8\%$	SMAP <u>V5</u>	<del>0.75</del> <u>0.79</u>	<del>5.15</del> <u>5.29</u>	<del>-2.35</del> <u>-2.44</u>
	AMSR2	0.47	<del>4.98</del> <u>5.19</u>	<del>-2.00</del> <u>-2.26</u>
	ASCAT	0.23	<del>5.01</del> <u>5.19</u>	<del>-1.82</del> <u>-2.17</u>
$\frac{d\Theta_{sat}}{\Theta_{sat}^{t-n}} \geq 12\%$	SMAP <u>V5</u>	<u>0.80</u>	<del>5.2</del> <u>5.32</u>	<del>-2.4</del> <u>-2.47</u>
	AMSR2	0.56	<del>5.01</del> <u>5.21</u>	<del>-2.1</del> <u>-2.32</u>
	ASCAT	0.36	<del>5.05</del> <u>5.23</u>	<del>-2.06</del> <u>-2.29</u>